Tectonics

RESEARCH ARTICLE
10.1029/2018TC005250

Key Points:
- Since 1.9 Ga, the NE Fennoscandia was characterized by a slow exhumation (1-2 m/Myr)
- Total denudation of the NE Fennoscandia since 1.9 Ga did not exceed ~3-5 km
- The Kola part of Fennoscandia experienced endogenous event and/or burial 360-300 Ma

Supporting Information:
- Supporting Information S1
- Table S1

Correspondence to:
R. V. Veselovskiy,
roman.veselovskiy@ya.ru

Citation:
Veselovskiy, R. V., Thomson, S. N., Arzamastsev, A. A., Botsyun, S., Travin, A. V., Yudin, D. S., et al. (2019). Thermochronology and exhumation history of the northeastern Fennoscandian Shield since 1.9 Ga: evidence from $^{40}Ar/^{39}Ar$ and apatite fission track data from the Kola Peninsula. *Tectonics*, *38*. https://doi.org/10.1029/2018TC005250

Received 22 JUL 2018
Accepted 31 MAY 2019
Accepted article online 26 JUN 2019

Thermochronology and Exhumation History of the Northeastern Fennoscandian Shield Since 1.9 Ga: Evidence From $^{40}Ar/^{39}Ar$ and Apatite Fission Track Data From the Kola Peninsula

Roman V. Veselovskiy[1,2], Stuart N. Thomson[3], Andrey A. Arzamastsev[4,5], Svetlana Botsyun[6], Aleksey V. Travin[7,8], Denis S. Yudin[7,8], Alexander V. Samsonov[9], and Alexandra V. Stepanova[10]

[1]Geological Faculty, Lomonosov Moscow State University, Moscow, Russia, [2]Institute of Physics of the Earth, Russian Academy of Sciences, Moscow, Russia, [3]Department of Geosciences, University of Arizona, Tucson, AZ, USA, [4]Institute of Precambrian Geology and Geochronology, Russian Academy of Sciences, Saint Petersburg, Russia, [5]Institute of Earth Sciences, Saint Petersburg State University, Saint Petersburg, Russia, [6]Department of Geosciences, University of Tuebingen, Tuebingen, Germany, [7]Sobolev Institute of Geology and Mineralogy Siberian Branch Russian Academy of Sciences, Novosibirsk, Russia, [8]Department of Geology and Geophysics, Novosibirsk State University, Novosibirsk, Russia, [9]Institute of Geology of Ore Deposits Petrography Mineralogy and Geochemistry, Russian Academy of Sciences, Moscow, Russia, [10]Institute of Geology, Karelian Research Centre, Russian Academy of Sciences, Petrozavodsk, Russia

Abstract Results from thermochronological studies have multiple applications to various problems in tectonics and landform evolution. However, up to now a lack of thermochronological data from the northeastern Fennoscandian Shield has complicated the interpretation of tectonothermal evolution of the region. Here, we use both new and previously published multimineral $^{40}Ar/^{39}Ar$ data (amphibole, mica, and feldspar) on the various Precambrian magmatic and metamorphic complexes to reconstruct the thermal history of NE Fennoscandia within the Kola Peninsula area in the interval 1900–360 Ma. Using the apatite fission track method as well as a numerical model of the heating-cooling process of northeastern Fennoscandia's upper crust, we have reconstructed its thermal evolution for the interval 360–0 Ma. According to our model, since Lapland-Kola orogenesis (1930–1905 Ma) northeastern Fennoscandia experienced a quasi-monotonous cooling with the average rate of ~0.15 °C/Myr, which is equal to an exhumation rate of ~1–2 m/Myr. New apatite fission track data and time-temperature modeling reveal a "hidden" endogenous thermal event in the NE Fennoscandia that took place between 360 and 300 Ma. This we attribute to an elevated geothermal gradient due to Baltica's drift over the African large low shear-wave velocity province in the lowest mantle and/or thermal blanketing by insulating Devonian-Carboniferous sedimentary/volcanic cover. Our model is further supported by evidence of Late Devonian-Carboniferous rifting in the East and South-Western Barents Basin, as well as various 360–300 Ma magmatic events within SW Fennoscandia and the Baltic countries.

1. Introduction

Northeastern Fennoscandia, especially the Kola Peninsula, is very poorly characterized by currently published thermochronological data. For this reason, the thermal evolution of this part of the Fennoscandian Shield remains poorly known. This problem becomes particularly acute when compared to southwestern and central Fennoscandia, the areas of Finland, Norway, and Sweden, which have been extensively studied using modern thermochronological methods, such as $^{40}Ar/^{39}Ar$ dating (Sandström et al., 2009; Söderlund et al., 2008) and detailed zircon, titanite, and apatite fission track analysis (Fossen et al., 2017; Hendriks et al., 2007; Ksienzyk et al., 2014). Published thermochronological models of SW and central Fennoscandia based on these data have led to tectonic history reconstructions (Japsen et al., 2016; Kohn & Gleadow, 2019; Hendriks et al., 2007; Murrell & Andriessen, 2004; Murrell, 2003; Redfield et al., 2005) that demonstrate contrasting amplitude of vertical movements since the Paleoproterozoic even for neighboring tectonic units.

Available estimates of the Phanerozoic denudation from the Kola part of the Fennoscandian Shield and the corresponding amplitudes of its vertical movements are largely ambiguous. Semiquantitative estimates of

the Phanerozoic erosion of sedimentary cover and Devonian intrusive bodies and diatremes show significant differences in the amplitude of the denudation of the area—from 0 km on the periphery of the Kola Peninsula up to 6 km in its central part (Hall, 2015). Reliable models of the Precambrian thermal history and quantitative estimates of the denudation volume of the Kola Peninsula are absent. Published thermochronological data, obtained by fission track analysis of apatite, titanite, and zircon from the Kola Superdeep Borehole (SG3; Hendriks et al., 2007; Kohn & Gleadow, 2019; Rohrman, 1995), are very local and thus likely do not reflect processes operating at the scale of the whole Kola Peninsula.

Recently, to test the hypothesis of a Mesozoic regional remagnetization event within the Fennoscandian Shield (Veselovskiy et al., 2013, 2016), we obtained apatite fission track (AFT) ages from samples taken from various depths of the Devonian Khibina pluton (Veselovskiy et al., 2015). These AFT data, together with computer modeling of the post-emplacement cooling of the Khibina massif, allowed us to model its tectonothermal evolution during the last 360 Myr. The results of this modeling showed post-Devonian denudation of the Khibina massif of around 5–6 km and that the mean geothermal gradient remained ~20 °C/km for at least the last 250 Myr. But this conclusion contradicts independent post-Devonian erosion estimates for the central part of the Kola Peninsula of ~1–2 km proposed by Hall (2015).

The main goal of this study is to produce quantitative model of the tectonothermal evolution of northeastern Fennoscandia. We use previously published and 12 new AFT results obtained on apatite from magmatic and metamorphic complexes of different age, widely distributed within the Kola Peninsula part of the shield. In addition, we present new $^{40}Ar/^{39}Ar$ ages from Paleoproterozoic dolerite and granitic dykes across the whole Kola Peninsula. These data have allowed us to construct the thermal history of the northeastern Fennoscandian Shield since ~1.9 Ga. This history begins with consolidation of the main Archean and Paleoproterozoic terranes and the cessation of metamorphism and includes such major tectonothermal events as the formation of the Kola Alkaline magmatic province ~400–360 Ma (Arzamastsev et al., 2017).

2. Geologic Setting and Sampling

2.1. Geological background

The northeastern Fennoscandian Shield, long regarded as an Archean craton, is a collisional orogen (Lapland-Kola Orogen, LKO) comprising mainly Archean terranes finally welded together in the Paleoproterozoic (Daly et al., 2001; Glebovitsky, 1997; Mitrofanov et al., 1995). Balagansky et al. (1998) divides the LKO into dispersed and accreted terranes. The dispersed terranes (Murmansk, Central Kola, Inari, and Belomorian, Figure 1) comprise fragments of a rifted Neoarchaean craton, reassembled in the Paleoproterozoic. The accreted terranes include the Lapland Granulite Terrane (known as the Lapland Granulite Belt), Umba Granulite Terrane, and Tersky Terrane, all composed of Paleoproterozoic juvenile crust generated in an island-arc setting (Balagansky et al., 1998; Daly et al., 1997; Huhma & Meriläinen, 1991). The oldest tonalite-trondhjemite-granodiorite gneisses (TTG) were formed around 2.95–2.90 Ga. These rocks are found within a Mesoarchean complex occupies the northwestern and the central parts of the Kola Peninsula. It comprises granitoids and volcanic and sedimentary rocks that underwent regional amphibolite and granulite metamorphism. In this terrane, abundant Neoarchean intracrustal structures, together with fragments of supracrustal rocks, are involved in linear NW-SE trending folds. The Keivy collage domain occupies almost the entire eastern part of the Central Kola terrane. The most conspicuous feature of this domain is the presence of voluminous anorogenic alkaline granites of 2.61–2.68 Ga, which intrude a supracrustal high-Al schist rock sequence metamorphosed to kyanite-sillimanite grade of the amphibolite facies. The Archean Murmansk terrane, which forms the northern part of the Kola Peninsula, consists of dominating oligoclase granite gneiss and migmatite, enderbite and charnockite. The Belomorian terrane consists largely of Neoarchean dome-fold and complex-fold structures reworked in the Paleoproterozoic. For the most part the terrane area is composed of granite-gneiss, migmatite, and gneiss containing amphibolite bodies.

The Paleoproterozoic rifting of the Archean Kola basement craton produced the NW-SE trending Pechenga-Imandra-Varzuga Volcanic Belt (Melezhik & Hanski, 2012; Mitrofanov et al., 1995), in which intense bimodal magmatism occurred over about 500 Myr (Sharkov & Smolkin, 1997). The Neoproterozoic belt comprises two major structures: the Pechenga and Imandra-Varzuga zones separated by a Neoproterozoic meridional thrust with a horizontal translation of around 100 km. The Pechenga zone is marked by a graben syncline

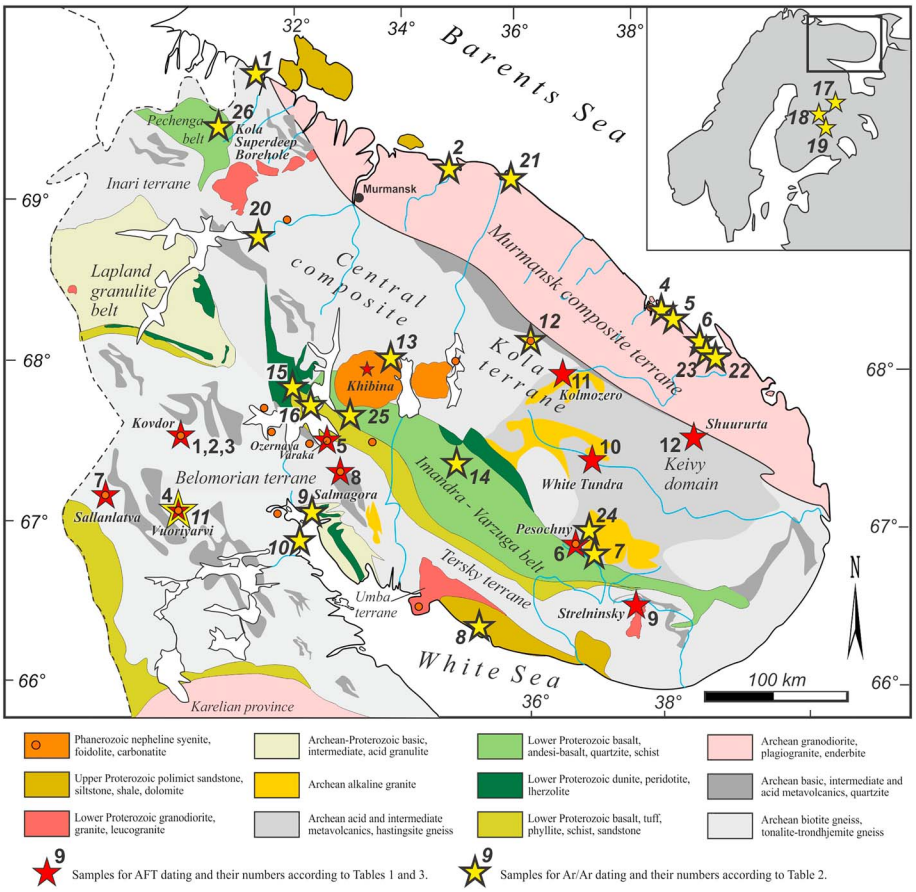

Figure 1. Sketch tectonic map of the Kola Peninsula showing sampling localities. The inset shows the position of Kostomuksha (17), Kaavi-Kuopio (19), and Lentiira-Kuhmo (18) kimberlites in the Fennoscandian Shield. $^{40}Ar/^{39}Ar$ data obtained from (Arzamastsev et al., 2009, 2017; Arzamastsev & Petrovsky, 2012; Nosova et al., 2015; O'Brien et al., 2007). AFT = apatite fission track.

filled with a stratified rhythmically alternating sequence of volcanic rocks and sedimentary deposits pierced by numerous ultrabasic layered intrusions, containing nickel and copper mineralization. The Imandra-Varzuga zone features the same structure and rock sequence. Magmatic activity directly related to the Pechenga-Varzuga Belt finished at 1.9 Ga. The final Proterozoic events are marked by Litsa-Araguba granitoid intrusions (Vetrin, 2014) that terminated at 1.75 Ga. This was followed by a 1.3 billion year-long amagmatic period which lasted until the Devonian. Since this time, the NE Fennoscandian Shield has been characterized by stable continental crust with a constant uplift tendency (Amantov et al., 1995; Amantov & Fjeldskaar, 2013). As a result, Mesoproterozoic and Neoproterozoic (Riphean and Vendian in Russian nomenclature) sedimentary rocks crop out in a few inland depressions. In the Phanerozoic, northeastern Fennoscandia was host to intense alkaline and carbonatite magmatism. The main magmatic events took place in the central and western parts of the Kola Peninsula at 380–360 Ma (Arzamastsev & Wu, 2014; Kramm et al., 1993; Kramm & Kogarko, 1994; Rukhlov & Bell, 2010) when giant agpaitic syenite complexes and 19 carbonatite intrusions were formed. Numerous tholeiitic dykes of Paleozoic age were found recently in the Murmansk block. According to geochronological data formation of these dykes occurred before the alkaline and carbonatite complexes (Arzamastsev et al., 2017).

2.2. Sampling

Apatite for fission track analysis was separated from rocks from both the Precambrian and Phanerozoic magmatic and metamorphic complexes (Table 1), widely spread over different parts of the northeastern

Tectonics

10.1029/2018TC005250

Table 1
Samples Used for Apatite Fission Track Investigation

NN	Sample no.	Depth relative to surface (m)	Latitude[a]	Longitude[a]	Locality	Rock name	Age (Ma)	Method	Reference
1	7/57	57	67°33′55″	30°26′12″	Kovdor carbonatite massif	Ijolite with apatite	378 ± 2	U-Th-Pb zircon, apatite	Amelin and Zaitsev (2002)
2	7/194	194	67°33′55″	30°26′12″	Kovdor carbonatite massif	Ijolite with apatite and titanite	378 ± 2	U-Th-Pb zircon, apatite	Amelin and Zaitsev (2002)
3	7/691.5	691.5	67°33′55″	30°26′12″	Kovdor carbonatite massif	Ijolite with apatite and titanite	378 ± 2	U-Th-Pb zircon, apatite	Amelin and Zaitsev (2002)
4	235/225	225	66°47′52″	30°08′15″	Vuoriyarvi carbonatite massif	Alkaline picrite with carbonate	369 ± 1	$^{40}Ar/^{39}Ar$, biotite	Arzamastsev et al. (2003)
5	7-OV	0	67°25′50″	32°57′41″	Ozernaya Varaka carbonatite massif	Melteigite	376 ± 3	Rb-Sr, mineral isochron	Kramm et al. (1993)
6	2969	0	67°07′05″	37°13′30″	Pesochny carbonatite massif	Ijolite with calcite and apatite	379 ± 3	$^{40}Ar/^{39}Ar$, biotite	A. A. Arzamastsev (personal communication, 2007)
7	31/200	200	66°44′48″	29°31′18″	Sallanlatva carbonatite massif	Ijolite	369 ± 2	U-Pb, zircon	Sitnikova et al. (2001)
8	731B	0	67°18′00″	33°30′00″	Salmagorsky carbonatite massif	Ijolite	375 ± 10	U-Pb Ca-Ti garnet	Kogarko et al. (1995)
9	226/79	0	66°42′12″	37°56′10″	Sliudyanka river, Strelninsky alkaline granite massif	Alkaline pegmatoid granite	2670 ± 8	U-Pb, zircon	Vetrin and Rodionov (2009)
10	457/59	0	67°20′49″	37°03′08″	Krasnoschel'e village, White Tundraalkaline granite massif	Plagiogranite	2674 ± 10	U-Pb, zircon	Vetrin and Rodionov (2009)
11	81/64	0	67°59′48″	36°43′55″	Kolmozero lake, West-Keivy domain	Tonalite, Archean basement	2733 ± 6	U-Pb, zircon	Kudryashov et al. (2013)
12	142/69	0	67°32′39″	38°16′57″	Shuururta mt., Keivy. Central Kola terrane	Garnet-biotite gneiss, Archean basement	~2750	—	Batieva (1976)

[a]Map datum WGS84.

Fennoscandia (Figure 1, red stars). Studied samples were taken from outcrops as well as from the drill cores. Note that the Kovdor massif is represented by three samples from different depths.

In this study we also present new $^{40}Ar/^{39}Ar$ ages from samples collected from Early Precambrian rocks within the different regions of the Kola Peninsula (Figure 1, yellow stars). Samples were taken from outcrops as well as from the Kola Superdeep Borehole (SG3). Details on these samples are listed in Table 2. Previously published $^{40}Ar/^{39}Ar$ data, which we use in the discussion, are also shown (Figure 1 and Table 2).

3. Methods

3.1. $^{40}Ar/^{39}Ar$ Dating

The $^{40}Ar/^{39}Ar$ isotope geochronological data were obtained at the Sobolev Institute of Geology and Mineralogy of the Siberian Branch of the Russian Academy of Sciences (Novosibirsk). Mineral grains for dating were handpicked under a binocular microscope from the 0.25- to 0.15-mm fraction of crushed rock. The samples were irradiated at the cadmium-lined channel of the VVR-K-type research reactor of the Institute of Physics and Technology at the Tomsk Polytechnic University. Stepwise heating experiments were conducted in an externally heated quartz vessel. The ^{40}Ar blank (20 min at 1200 °C) was no higher than $n \times 10^{-10}$ ncm^3. The extracted argon was purified using Zr-Al SAES getters. Argon isotope composition was measured with a Micromass noble gas 5,400 mass spectrometer. Calculated $^{40}Ar/^{39}Ar$ ages are reported with $\pm 1\sigma$ uncertainties.

3.2. Fission track Dating

Apatite grains of >0.2 mm size were mounted in epoxy resin, alumina polished, and spontaneous fission tracks (FTs) revealed by etching with 5.5 M HNO_3 at 20 °C for 20 s. Samples were analyzed using the external detector method (Gleadow, 1981) using very low uranium, annealed muscovite mica detectors, and irradiated at the Oregon State University Triga Reactor, Corvallis, United States. The neutron fluence was monitored using European Institute for Reference Materials and Measurements (IRMM) uranium-dosed glass IRMM 540R. After irradiation, induced tracks in the mica external detectors were revealed by etching with 48% hydrofluoric acid (HF) for 18 min. Spontaneous and induced FT densities were counted using an Olympus BX61 microscope at 1250X magnification with an automated Kinetek Stage system. Apatite FT lengths and Dpar values were measured using FTStage software, an attached drawing tube, and digitizing tablet supplied by Trevor Dumitru of Stanford University calibrated against a stage micrometer. Central ages (Galbraith, 2005; Galbraith & Laslett, 1993), quoted with 1σ uncertainty, were calculated using the IUGS recommended zeta-calibration approach of Hurford and Green (1983). An apatite IRMM 540R zeta-calibration factor of 368.1 ± 14.9 was obtained by repeated calibration against a number of internationally agreed age standards including Durango and Fish Canyon apatite according to the recommendations of Hurford (1990).

3.3. Thermal History Modeling

To constrain the thermal history of the studied samples consistent with apatite FT (AFT) ages and track lengths distribution, we used HeFTy software version 1.8.6 (Ketcham, 2005). HeFTy is a popular thermal history modeling software, in which formalized statistical hypothesis tests assess the goodness-of-fit between the input AFT data and AFT data predicted from many thousands of time-temperature (t-T) paths according to the Ketcham et al. (2007) AFT annealing model (Vermeesch & Tian, 2014). The output of the model is two t-T envelopes (Figure 4): the broader envelope being the range within which any thermal history cannot be excluded by the measured data (acceptable fit); the narrower envelope being the range that is supported by the measured data (good fit). The merit values used are “0.05” for acceptable fit and “0.5” for good fit. For all cases, simulations were run until 100 good fit paths were found. We apply a present day mean annual surface temperature for the Kola Peninsula of Tann = 0 °C (Met Office: www.metoffice.gov.uk/).

Additionally, we applied multidiffusion domain modeling (Lovera et al., 1989) for $^{40}Ar/^{39}Ar$ stepwise heating data, obtained on the K-feldspar from the granite sample taken from at a depth of 9.5 km (35547), with the aim to get more constrains for the t-T model (Figure 2j).

Tectonics

10.1029/2018TC005250

Table 2
$^{40}Ar/^{39}Ar$ Data: Currently Obtained and Previously Published

NN	Sample no.	Latitude[a]	Longitude[a]	Locality	Rock name	Plateau age (Ma)	Mineral	Reference
1	A03-20	69°30′08″	31°15′30″	Pechenga area	Dolerite	381.0 ± 5.5	Biotite	Arzamastsev et al. (2009)
2	A09-08	69°11′38″	35°07′43″	Teriberka settl.	Dolerite	374.3 ± 4.1	Plagioclase	Arzamastsev et al. (2017)
3	A99-1	67°33′37.1″	33°26′39.7″	Apatity area	Alkaline lamprophyre	388.1 ± 5.8	Amphibole	Arzamastsev et al. (2009)
4	19-2013	68°15′40.8″	38°44′4.1″	Ivanovka fiord	Dolerite	378.0 ± 5.6	Feldspar	Arzamastsev et al. (2017)
5	17-2013	68°13′12.9″	38°49′35.0″	Ivanovka fiord	Dolerite	382.8 ± 5.6	Feldspar	Arzamastsev et al. (2017)
6	14-2013	68°03′16.9″	39°29′50.7″	Ostrovnoy settlement	Dolerite	380.8 ± 5.8	Plagioclase	Arzamastsev et al. (2017)
7	2969	67°04′07.9″	37°04′19.1″	Varzuga river	Foidolite	379.0 ± 3.0	Phlogopite	Arzamastsev et al. (2009)
8	77/258	66°25′39.7″	35°35′47.0″	Tersky coast	Kimberlite	376.1 ± 1.3	Phlogopite	Arzamastsev et al. (2009)
9	A05-19A	67°07′24.6″	32°26′51.1″	Kandalaksha	Alkaline lamprophyre	378.5 ± 3.9	Phlogopite	Veselovskiy et al. (2013)
10	A05-13	67°06′52.2″	32°29′12.6″	Kandalaksha	Alkaline lamprophyre	380.8 ± 4.0	Phlogopite	Veselovskiy et al. (2013)
11	235/225	66°47′52.0″	30°08′14.9″	Vuoriyarvi carbonatite massif	Alkaline picrite with carbonate	369.1 ± 0.9	Phlogopite	Arzamastsev et al. (2003)
12	A09-06	69°07′08″	36°06′27″	Dalnie Zelentsy settlement	Dolerite	367.6 ± 5.6	Feldspar	Arzamastsev et al. (2017)
13	1635/352	67°51′20.3″	34°05′36.9″	Khibina alkaline massif	Alkaline picrite	363.4 ± 2.5	Phlogopite	Arzamastsev et al. (2009)
14	L03-18	67°17′48.7″	34°13′53.5″	Ingozero alkaline massif	Melilitolite	380.1 ± 5.5	Phlogopite	Arzamastsev et al. (2009)
15	A02-01	67°45′49.7″	32°45′54.9″	Monchegorsk area	Gabbro-dolerite	1149.9 ± 13.4	Biotite	This study
16	1250	67°38′08.0″	32°47′23.2″	Voche-Lambina area	Gabbro-dolerite	1160.8 ± 12.9	Biotite	This study
17	Ko	64°41′06″	30°39′35″	Kostomuksha	Lamproite	1224 ± 24	Phlogopite	Nosova et al. (2015)
18	Le	64°31′48.4″	29°33′52.6″	Lentiira-Kuhmo	Lamproite	1204 ± 4	Phlogopite	O'Brien et al. (2007)
19	KK	64°14′44.3″	29°47′56.3″	Kaavi-Kuopio	Lamproite	1203 ± 3	Phlogopite	O'Brien et al. (2007)
20	A03-03	68°36′28.7″	31°45′59.1″	Verkhnetulomsky area	Ca-alkaline lamprophyre	1767 ± 18	Biotite	This study
21	Ca-552-3	69°07′25.8″	36°02′52.5″	Dalnie Zelentsy settlement	Poikilo-ophitic dolerite	1857 ± 20	Biotite	This study
						1772 ± 11		
22	549	68°02′19.5″	39°33′46.3″	Gremikha area	Nepheline pyroxenite	1955.0 ± 10.8	Biotite	This study[b]
						1370.9 ± 8.2	Plagioclase	This study[b]
						1230.2 ± 6.6		
23	526-03	68°02′28.1″	39°33′21.4″	Gremikha area	Pyroxenite	2020.0 ± 6.5	Biotite	This study[b]
						1814.9 ± 6.0		
24	AR-44	67°04′10.2″	37°05′53.5″	Varzuga river	Pyroxenite	2057 ± 10	Amphibole	This study
	99-1	69°23′46.39″	30°36′31.20″	Kola Superdeep Borehole (SG3)	Granite, Litsa-Araguba dyke	1762 ± 9	Zircon	Vetrin et al. (2002)
25					(present-day surface)	1755.0 ± 2.9	Biotite	This study[c]
						1526.3 ± 4.3	K-Feldspar	This study[c]
26	35547	69°23′46.39″	30°36′31.20″	Kola Superdeep Borehole (SG3)	Granite, Litsa-Araguba dyke	1765 ± 2	Zircon	Kola Superdeep (1998)
					(9.5 km depth)	1431.3 ± 3.0	Biotite	This study[c]
						~1431	Muscovite	This study[c]
						~350 ± 50	K-Feldspar	This study[c]

[a]Map datum WGS84. [b]Sample from M.N.Petrovsky collection. [c]Samples from V.R.Vetrin collection.

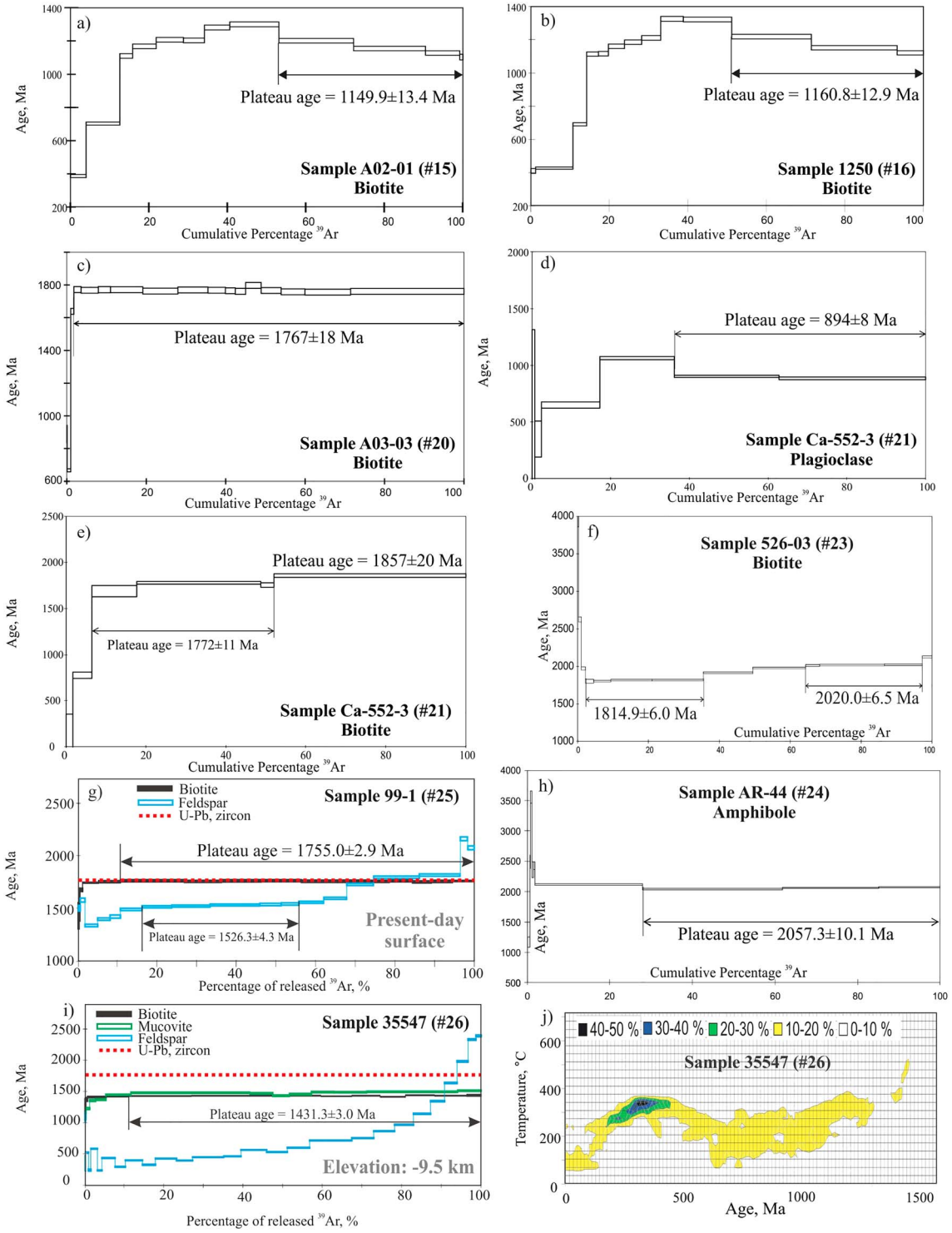

Figure 2. $^{40}Ar/^{39}Ar$ dating results (a–i) and the thermal history model for sample 35547 (#26), calculated using the thermally activated multidomain diffusion model of Lovera et al. (1989) for $^{40}Ar/^{39}Ar$ stepwise heating data, obtained on the potassium rich feldspar (j). Sample numbers correspond to Table 2.

4. Results

4.1. $^{40}Ar/^{39}Ar$ Data

The age of dolerites was determined by $^{40}Ar/^{39}Ar$ dating of biotite from two samples taken from dykes in a swarm that constitute a band (20 × 40 km in size) mapped in the Voche-Lambina domain (Figure 1). The obtained age spectra for biotite samples A02-01 (Figure 2a) and 1250 (Figure 2b) are characterized by intricate patterns: the stepwise increase in values begins with an age of 409–386 Ma, followed first by relatively elevated values and then by a plateau with ages of 1150 ± 13 and 1161 ± 13 Ma in the high-temperature part of the spectrum. The low-temperature regions of the spectra reflect influence of the adjacent Khibina Devonian alkaline massif. The obtained ages correspond to an Rb-Sr age determination of the same dyke – 1176 ± 28 Ma (Arzamastsev et al., 2009). These data are similar to K-Ar and $^{40}Ar/^{39}Ar$ ages from lamproite dykes in the Kostomuksha area—1193 ± 20 Ma (Wiersberg, 2001) and 1224 ± 24 Ma (Nosova et al., 2015), as well as $^{40}Ar/^{39}Ar$ dating of kimberlites of the Kaavi-Kuopio in Finland (O'Brien et al., 2007). All the above $^{40}Ar/^{39}Ar$ data were repeated by Rb-Sr analyses (Arzamastsev et al., 2009).

A dyke swarm found in the Central Kola Archean domain in the Verkhnetulomsky district (Figure 1) comprises several subvertical dykes made of Ca-alkaline lamprophyre. Biotite $^{40}Ar/^{39}Ar$ dating of sample A03-03 from the core zone of a 3-m thick dyke yielded a plateau age of 1767 ± 18 Ma (Figure 2c).

Biotite sample Ca-552-3 taken from the central zone of subhorizontal sill of poikilo-ophitic dolerite intruded in Archean gneisses of the Murmansk terrane near the settlement Dalnie Zelentsy (Figure 1), yielded an $^{40}Ar/^{39}Ar$ age spectrum with two well-defined plateaus: at 1857 ± 20 Ma and 1772 ± 11 Ma (Figure 2e). The older, higher-temperature plateau matches an Sm-Nd age determination of the same sill—1908 ± 60 Ma (Arzamastsev et al., 2009), and more precise zircon and baddeleyite U-Pb ages of 1863 ± 11 and 1849 ± 11 Ma (Fedotov et al., 2012). It should be noted that the age spectrum of a plagioclase from the same sample Ca-552-3 reveals a plateau at 894 ± 8 Ma (Figure 2d).

Sample AR-44 was collected from a pyroxenite body close to the Pesochny Paleozoic carbonatite massif, which intrudes the volcanic-sedimentary complex of the Imandra-Varzuga belt (Figure 1). The obtained amphibole age spectrum begins with an unclear lower-temperature part, which is followed by a plateau with age of 2057 ± 10 Ma in the high-temperature part of the spectrum (Figure 2h).

The pyroxenite sample 526-03 from the Gremikha area (Figure 1) shows a biotite step-heating age spectrum with two plateaus corresponding to the ages 2020.0 ± 6.5 and 1814.9 ± 6.0 Ma (Figure 2f), which possibly mark two cooling events.

Comparative analysis of two granite samples representing the Litsa-Araguba complex in the northwestern part of the Kola Peninsula (Figure 1) using the $^{40}Ar/^{39}Ar$ stepwise heating method reveals significant differences in their thermal history. Sample 35547 was taken from the core of the Kola Superdeep Borehole (SG3) at a depth of 9.5 km and sample 99-1 from a granite dyke on the present-day surface. Previously U-Pb zircon ages from these samples (Kola Superdeep, 1998; Vetrin et al., 2003) yielded ages of 1765 ± 2 and 1762 ± 9 Ma, respectively (Table 2). An $^{40}Ar/^{39}Ar$ age obtained for biotite from sample 99-1 (1755.0 ± 2.9 Ma) practically coincides with the time of rock crystallization (Figure 2g), but the $^{40}Ar/^{39}Ar$ age of the intermediate temperature plateau in the spectrum of feldspar from the same sample (1526.3 ± 4.3 Ma) can be considered as evidence for a low-temperature (~150–250 °C) event that did not affect the K-Ar isotope system of biotite.

Stepwise heating of three mineral fractions separated from granite sample 35547 (9.5-km depth) reveals two well defined plateaus for muscovite and biotite (1431.3 ± 3.0 Ma); the feldspar shows no clear plateau, but the youngest ages imply K-Ar system closure by ~350 ± 50 Ma (Figure 2i). This pattern can be explained in thermal history terms: (1) For about 260 Myr after granite crystallization at ~1765 Ma the rock had a temperature ~450–500 °C and K-Ar system in micas were opened; (2) at ~1431 Ma the K-Ar system in micas closed due to a cooling event; and (3) K-Ar system in feldspar reveals a final cooling event at ~400–300 Ma. Application of multidomain thermally activated diffusion modeling to the K-feldspar data from the deep sample 35547 (Lovera et al., 1989; Figure 2j) supports this secondary heating/cooling between 400 and 300 Ma. We postulate that this heating is linked with Middle-Late Devonian activity during the Kola Alkaline province formation.

Table 3
Apatite Fission Track Data

NN	Sample no.	No. of crystals	Track Density ($\times 10^6$ tracks/cm^2; no. of tracks) ρ_s (N_s)	ρ_i (N_i)	ρ_d (N_d)	Mean D_{par} (μm)	Mean U (ppm)	Age dispersion ($P\chi^2$)	Central age (Ma; ±1σ)	Apatite mean track length (μm ± 1 s.e.; no. of tracks)	Standard deviation (μm)
1	7/57	12	1.538 (1132)	1.205 (887)	1.383 (4427)	2.41	13.1	<0.01% (99.1%)	316.9 ± 19.7	13.99 ± 0.12 (100)	1.17
2	7/194	20	1.861 (2204)	1.401 (1659)	1.373 (4392)	3.09	15.3	<0.01% (99.8%)	327.3 ± 17.7	13.99 ± 0.13 (100)	1.25
3	7/691.5	20	1.058 (1354)	0.9012 (1165)	1.362 (4358)	3.44	10.0	<0.01% (99.9%)	285.0 ± 16.8	13.16 ± 0.16 (100)	1.56
4	235/225	17	0.3389 (288)	0.2447 (208)	1.313 (4203)	2.38	2.8	<0.01% (>99.9)	326.2 ± 32.9	14.37 ± 0.15 (52)	1.06
5	7-OV	18	0.9792 (1128)	0.8047 (927)	1.394 (4461)	3.32	8.7	<0.01% (99.9%)	304.9 ± 18.9	14.22 ± 0.14 (108)	1.49
6	2969	20	0.2115 (268)	0.1736 (220)	1.265 (4047)	3.22	2.1	<0.01% (>99.9%)	277.6 ± 28.0	14.69 ± 0.14 (60)	1.09
7	31/200	17	0.5492 (580)	0.4479 (473)	1.254 (4013)	2.61	5.4	<0.01% (>99.9%)	277.0 ± 21.0	14.42 ± 0.12 (73)	1.04
8	731B	20	0.6539 (837)	0.5172 (662)	1.281 (4099)	2.52	6.1	<0.01% (99.9%)	291.4 ± 19.7	14.29 ± 0.11 (110)	1.15
9	226/79	20	0.5398 (684)	0.4143 (525)	1.329 (4254)	1.80	4.7	<0.01% (>99.9%)	311.1 ± 22.5	13.00 ± 0.43 (16)	1.67
10	457/59	20	1.402 (1319	1.151 (1083)	1.297 (4151)	1.81	13.3	<0.01% (99.9%)	284.4 ± 17.0	13.61 ± 0.12 (100)	1.19
11	81/64	20	2.680 (3053)	1.914 (2180)	1.351 (4323)	2.12	21.2	<0.01% (95.4%)	339.2 ± 17.5	13.44 ± 0.15 (100)	1.45
12	142/69	2	1.969 (252)	1.672 (214)	1.340 (4289)	2.79	18.7	<0.01% (99.9%)	284.1 ± 29.1	12.87 ± 0.27 (31)	1.46

Notes. (i) Analyses by external detector method using 0.5 for the $4\pi/2\pi$ geometry correction factor; (ii) ages calculated using dosimeter glass: IRMM540R with $\zeta_{540R} = 368.1 \pm 14.9$ (apatite); (iii) $P\chi^2$ is the probability of obtaining a χ^2 value for ν degrees of freedom where ν = no. of crystals − 1; (iv) s.e. = standard error of the mean; (v) U ppm calculated from induced track density relative to IRMM540R glass with 15 ppm U.

Finally, numerous $^{40}Ar/^{39}Ar$ geochronological data from dolerite and alkaline dykes scattered throughout the whole Kola Peninsula were obtained during our previous work (Figure 1 and Table 2; Veselovskiy et al., 2013; Arzamastsev et al., 2017). Most of obtained $^{40}Ar/^{39}Ar$ ages (plagioclase, feldspar and mica) show well-defined plateaus which fall within 390–365 Ma time span.

4.2. AFT Data

Twelve samples yield AFT central ages ranging from 339.2 ± 17.5 Ma to 277.0 ± 21.0 Ma (1σ uncertainty), with a mean age value of 302 ± 12 Ma (Table 3 and Figure 3). AFT ages of the Kovdor massif samples, which were taken from depths between 57 and 691.5 m, are statistically indistinguishable; however, the deepest sample (7/691.5) has a younger AFT central age. In general, the obtained AFT ages for most of the samples are statistically indistinguishable within 1σ uncertainty.

Mean track lengths vary between 14.69 ± 0.14 and 12.87 ± 0.27 μm; the most reliable ($n > 100$) mean track length distributions were obtained for seven samples (Table 3). Track length distributions for all samples were unimodal (Figure 4), which indicates monotonic moderate to fast cooling without periods of long residence within the partial annealing zone.

Complete AFT data including individual grain age data, track length data, and D_{par} values are presented in supporting infromation Table S1.

5. Discussion

Precambrian tectonic evolution of the northeastern Fennoscandian Shield involved several stages of plume-lithospheric processes and phases of the Archean and Paleoproterozoic rifting, culminated in the amalgamation of the main terranes at 1.9–1.8 Ga, coinciding with the Lapland-Kola and Svecofennian orogeny. Following this, an amagmatic period lasted until the Devonian time. During this time, only a few minor manifestations of magmatic activity are known related to far-field tectonomagmatic events on the southern margins of the Fennoscandian Shield.

Isotope geochronology is one of the few quantitative tools available to reconstruct the Proterozoic thermal history of the Kola part of Fennoscandia. Here we used the $^{40}Ar/^{39}Ar$ dating method on the minerals amphibole, biotite, muscovite, and plagioclase, with the closure temperatures of approximately 600–400, 400–350, 350–300, and 350–150 °C, respectively (Reiners et al., 2005). To simplify our model, we use the mean values of the listed closure temperatures: 500 (amphibole), 350 (biotite and muscovite), 250 °C (feldspar, plagioclase). Post-Devonian thermal history reconstructions were made using AFT analysis, which provides

Figure 3. Distribution of the apatite fission track ages with sample numbers on the right. Provenance names and isotopic ages of the analyzed rocks are reported too. Published apatite fission track data from the Khibina pluton (Veselovskiy et al., 2015) are shown for comparison.

information on low-temperature thermal history (<~120 °C) through application of numerical time-temperature modeling.

5.1. Post-Svecofennian Thermal History (1.86 – 0.36 Ga)

5.1.1. Available $^{40}Ar/^{39}Ar$ Data Set

Our new and published $^{40}Ar/^{39}Ar$ isotope data age constraints of 2.06, 1.86, 1.77, 1.22, and 1.16 Ga (Table 2), except for 400–360 Ma, record major tectonomagmatic events, which took place beyond or in the marginal zones of the northeastern Fennoscandian Shield. Noteworthy is that most of the $^{40}Ar/^{39}Ar$ age determinations are verified by Rb-Sr isochron or U-Pb data (Arzamastsev et al., 2009), except for the oldest age of 2.06 Ga. Whereas the majority of $^{40}Ar/^{39}Ar$ data indicate the closure time of K-Ar isotope system immediately after crystallization, the amphibole 2.06 Ga age from metamorphosed pyroxenite likely reflects the time of regional high-grade metamorphism seen throughout the Imandra-Varzuga belt. Temporal coincidence of $^{40}Ar/^{39}Ar$ and precise U-Pb dating of baddeleyite for the 1.86 Ga sills (Veselovskiy et al., 2019) and the other $^{40}Ar/^{39}Ar$ and Rb-Sr data for the most of dykes supports relatively rapid cooling of sills and dykes below the closure temperature of K-Ar system. Available $^{40}Ar/^{39}Ar$ data set appears to suggest that all dykes and basement rocks throughout the whole Kola area retain primary temperature regime, which did not exceed 350 °C. Starting point of this regime is marked by age determination obtained for 2.06 Ga pyroxenite or, using the more precise and reliable $^{40}Ar/^{39}Ar$ and U-Pb data, for the 1.86 Ga sill (1857 ± 20 Ma, Ca-552-3). This period corresponds to termination of post-Svecofennian metamorphic events, which had an effect on the most part of the northeastern Fennoscandian Shield (Early Precambrian of the Baltic Shield, 2005).

It is important to note that thermal effects of Devonian alkaline magmatism were localized and did not significantly affect the temperature regime of the whole Kola area. An example is the 1.17 Ga dyke swarm (Figure 1, A02-01), which is located 20 km from the large Paleozoic Khibina agpaitic massif, the $^{40}Ar/^{39}Ar$ spectra from which are largely undisturbed by this event (Figure 2a). Extremely narrow contact zones, which do not exceed dozen of meters (Arzamastsev et al., 2011; Kozlov & Arzamastsev, 2015), are additional arguments in favor of local thermal effect of the Devonian alkaline intrusions on the Precambrian basement.

We use all the data discussed above to construct a time-temperature model of the NE Fennoscandia at about 1.9–1.8 Ga. A summary is given below:

1. The present-day surface rocks were cooled to below 350 °C very quickly following their crystallization about 1.86–1.77 Ga, as inferred from the coincidence of the $^{40}Ar/^{39}Ar$ ages from amphibole and micas and U-Pb, Sm-Nd, and Rb-Sr ages.
2. The present-day surface rocks, representing two different tectonic units (Murmansk and Central Kola terranes) cooled to below 250 °C at different times, 0.89 and 1.53 Ga, respectively.
3. Rocks from the Kola Superdeep Borehole at a depth of 9.5 km cooled to below 350 °C at 1.43 Ga and to below 250 °C at 400–300 Ma.

5.1.2. First-Order Geothermal Gradient Estimation

Direct interpretation of this $^{40}Ar/^{39}Ar$ data set in the tectonic terms, such as the amplitude of exhumation or burial, requires knowledge of the geothermal gradient through time. To estimate the geothermal gradient to a first order, we evaluated the pressure of the magma at the time of poikilo-ophitic dolerite sill (Ca-552-3) emplacement using clinopyroxenes (Nimis, 1999; Putirka, 2008) and obtained a value of 1.3 ± 0.4 kbar, which corresponds to a depth of 3.9 ± 1.2 km. If this sill was emplaced in the surrounding rocks which had the temperature between 350 and 250 °C, then the first-order estimation of the geothermal gradient for this area ~1.86 Ga is about 75 °C/km. It should be noted that this value has considerable uncertainty because of the errors of the depth (d) and temperature (T) estimations: from 49 °C/km (d = 5.1 km, T = 250 °C) up to 129 °C/km (d = 2.7 km, T = 350 °C).

5.1.3. Time-Temperature and Exhumation Model of the Kola Peninsula Area 1.86–0.36 Ga

Our proposed time-temperature model for the studied area for Paleoproterozoic and Early Phanerozoic time (1.9–0.4 Ga) is shown on Figure 5a.

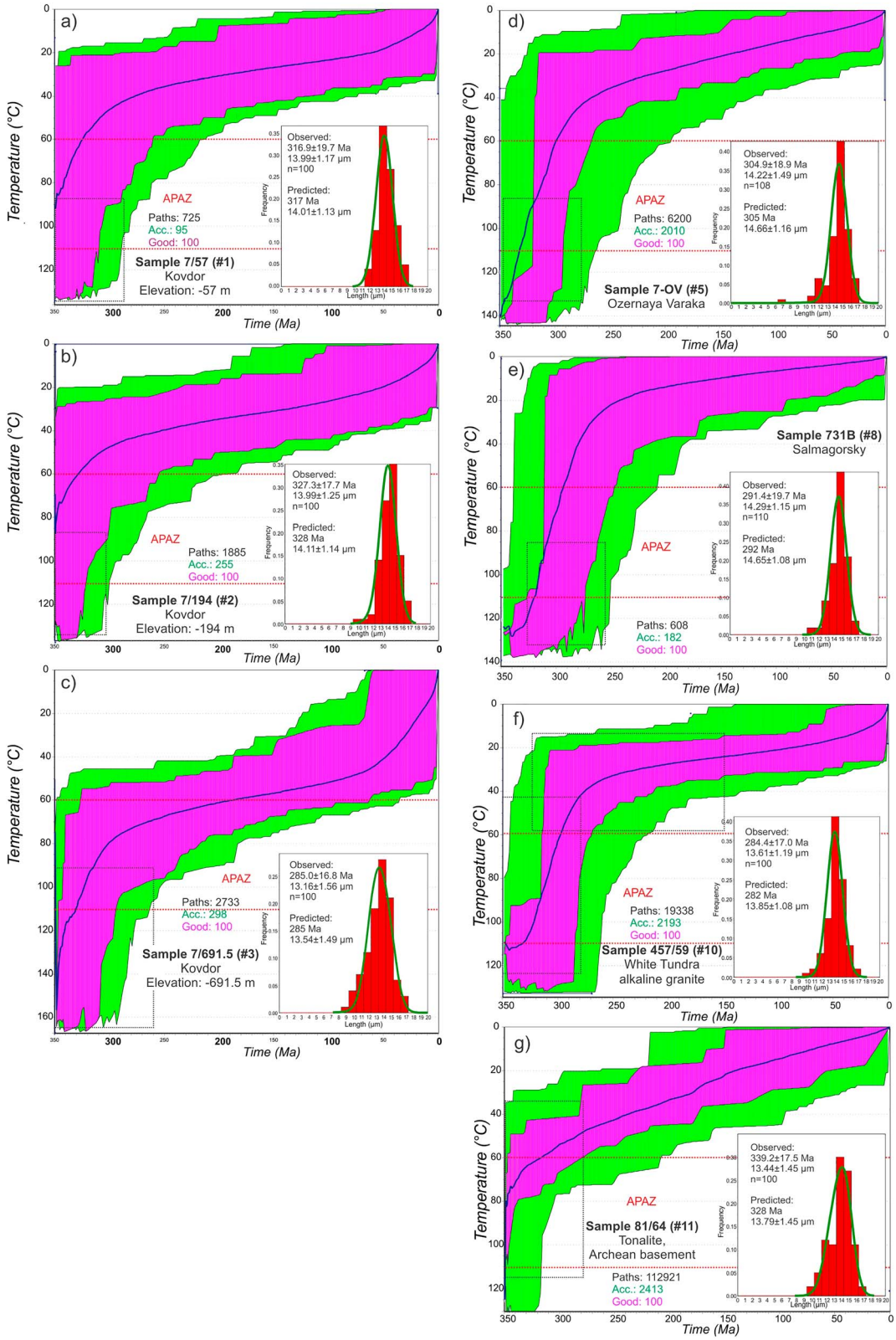

Figure 4. Results of the thermal modeling showing time-temperature envelopes that best predict the measured apatite fission track (AFT) age and track length data. The measured track length distribution histograms (red) and predicted length distribution (green line) are shown on the separate plot. Dashed boxes are constraint boxes.

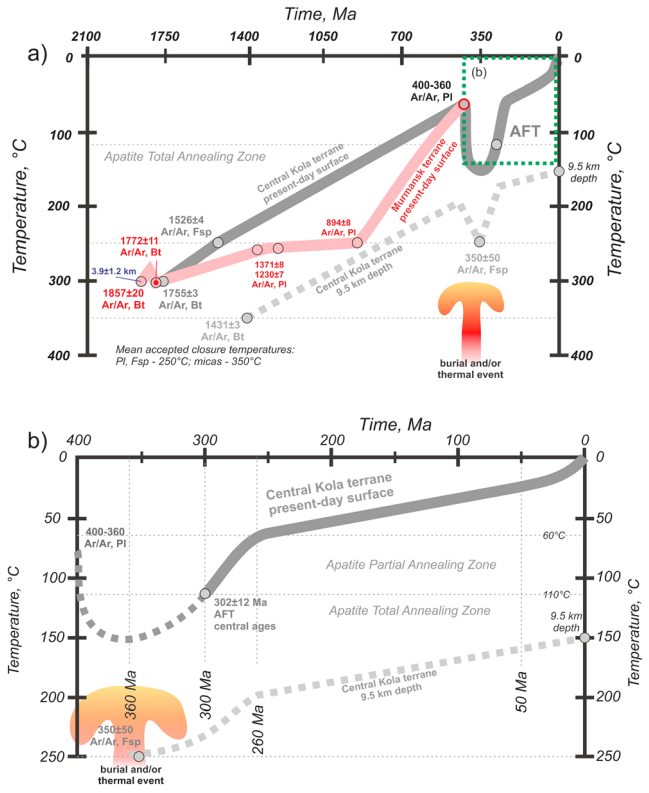

Figure 5. Proposed time-temperature (t-T) model of the Kola part of the Fennoscandian Shield for the last 1.9 Gyr including AFT data on the Khibina massif (Veselovskiy et al., 2015). (a) The t-T model is given for two tectonic units—Central Kola terrane (grey curves) and Murmansk terrane (pink curve). (b) Detailed t-T model for the 400–0 Ma time interval. AFT = apatite fission track.

The Kola Peninsula contains two main tectonic units, which have different structure and, possibly, thermal history: the Archean Murmansk terrane (craton) and the Proterozoic Central Kola terrane. We therefore constructed separate time-temperature trends for each terrane (Figure 5a). The pink curve corresponds to the present-day surface rocks of Murmansk terrane and starts at a point defined by data from the sample Ca-552-3, that includes coeval biotite $^{40}Ar/^{39}Ar$, and baddeleyite U-Pb ages (Veselovskiy et al., 2019) within uncertainties, and a depth value estimated by geothermobarometry. Then, K-Ar system in biotite was partially disturbed at about 1772 Ma, which we interpret to be a result of secondary heating and subsequent cooling related to a 1.77 Ga magmatic event. The next key point of the trend is the plagioclase $^{40}Ar/^{39}Ar$ age of 894 Ma from the same sample. This age can be interpreted in two possible ways: slow cooling the rocks below 250 °C due to exhumation or because of secondary heating. As this age value does not correspond to any known tectonomagmatic events within the Kola Peninsula, we prefer the first explanation. The curve ends at 400–360 Ma point, marked by numerous $^{40}Ar/^{39}Ar$ ages obtained for plagioclase from the dykes and plutons of the Kola Alkaline province. The point is situated relatively close to the surface because the geological and geophysical data indicate that the present-day level of Devonian intrusions corresponds to a depth of not more than a few kilometers at the time of their emplacement (Arzamastsev et al., 2000; Hall, 2015).

The Paleoproterozoic and early Phanerozoic thermal history of the Central Kola terrane of Fennoscandian Shield is represented on Figure 5a in greyish colors. The solid curve represents the t-T history of the present-day surface rocks, and the dashed line the rocks which were sampled at a depth of 9.5 km from the Kola Superdeep Borehole drill cores. First, we consider the present day surface rocks (solid grey curve). After the granite dyke emplacement about 1755 Ma, the rocks pass through the 250 °C isotherm ~1526 Ma and slowly cooled until 400 Ma. A granite dyke at a depth of 9.5 km was emplaced ~1765 Ma (Table 2) that cooled below 350 °C about 1431 Ma (dashed curve). The next cooling stage took place about 350 ± 50 Ma and is recorded by closure of the K-Ar system in feldspar (cooling below 250 °C). We propose that this stage was connected with thermal relaxation following the magmatic activity linked with a formation of the Kola Alkaline province, which almost fully reset the K-Ar system in feldspar. Further, the t-T trend goes to the point 0 Ma/150 °C—the present-day temperature at a depth of 9.5 km (Kola Superdeep, 1998).

In total, the thermal history of the NE Fennoscandia over the 1.9–0.4 Ga time interval is uneventful. The observed discrepancy between t-T paths of the Murmansk and Central Kola terranes can be linked with slightly different thermal and, possibly, exhumation history of these tectonic units, even for small blocks within each of them. For instance, the plagioclase $^{40}Ar/^{39}Ar$ data from samples 549 and Ca-552-3, separated by distance of 200 km, reflects at least three cooling events—1371, 1230, and 894 Ma, respectively. According to our model, the average estimated rate of cooling of rocks over this time interval did not exceed ~0.15 °C/Myr. To a first-order, total exhumation between 1.86 and 0.40 Ga can be estimated at about 2–3 km, which corresponds to a very slow average exhumation rate of 1–2 m/Myr.

5.2. Post-Devonian (360–0 Ma) Thermal and Exhumation History Based on AFT Data and t-T Modeling

We reconstructed the thermal history for this time interval using low-temperature AFT thermochronology. We only obtained AFT data from the Central Kola terrane. However, there is no evidence supporting any Phanerozoic large-scale vertical movements between the Mumansk and Central Kola terranes, so all the following conclusions can be extended on the whole Kola Peninsula area. However, we clearly understand

that further thermochronological research within the Murmansk terrane area would be need to fully confirm this.

Inverse modeling was performed using AFT data from all twelve studied samples, but we present only the most robust results from seven samples which contained ≥100 measured confined track lengths. Modeling results show that all studied samples have similar thermal histories (Figure 4). All the best fit t-T paths indicate these samples were cooled below ~110°C at about 300 Ma and cooled relatively fast through the apatite partial annealing zone to ≤~60 °C by 260 Ma. After that, the rocks cooled slowly until reaching their present temperatures. These t-T models match recently published AFT constrained t-T models of the Khibina pluton (Veselovskiy et al., 2015) implying a common Phanerozoic thermal history.

Based on the results of AFT t-T modeling (Figure 4), the thermal history of the rocks of the present-day surface of the Kola Peninsula consists of two stages:

1. ~320–260 Ma—moderate cooling from 110 to 50–40°C at a rate of about 1°C/Myr;
2. ~260–0 Ma—slow cooling from 50 to 40°C to 0°C at a rate of ~0.1–0.2°C/Myr.

In some cases, the best fit t-T paths show a third cooling event in the interval 50–0 Ma (Figures 4a, 4b, 4c, and 4f), during which there was an increase in the rate of rock cooling down to modern temperatures with a cooling rate ~0.4°C/Myr. We believe that this stage is not tectonic in nature but is the result of a global decrease in the surface temperature in the Cenozoic (Zachos et al., 2001, 2008); this issue was discussed in detail in Veselovskiy et al. (2015).

The tectonic interpretation of the second stage of the Kola thermal history is relatively straightforward. Assuming a geothermal gradient of ~20 °C/km for this time interval (Veselovskiy et al., 2015), at the beginning of this cooling stage ~260 Ma the rocks of the present-day surface were located at a depth of ~2 to 3 km. During the Mesozoic the rocks underwent slow exhumation with an average rate ~5–10 m/Myr: a value characteristic of denudation rates in ancient cratonic regions. For example, the Canadian Shield shows an average denudation rate of 2.5 m/Myr for the last 1.7 Ga (Flowers et al., 2006), and during the Mesozoic and Cenozoic—2–8 m/Myr (Peulvast et al., 2009). The rate of the Kola exhumation also agrees with an independent estimate of total denudation from the Kola Peninsula area during the Mesozoic-Cenozoic, which is about 1 km (Hall, 2015).

The more intensive cooling stage ~320–260 Ma has several possible causes: (1) exhumation related to tectonic uplift, (2) thermal relaxation (in situ cooling) of the upper crust after the Kola Devonian alkaline province magmatism, or (3) decrease of the heat flow throughout the Kola Peninsula area after 320 Ma. We consider each these three possibilities in detail below.

5.2.1. Scenario #1: Cooling Due to Exhumation Only

At about 320 Ma the rocks of the present-day surface passed through the 110 °C isotherm, which would have been located at a depth of about 5–6 km, and then were exhumed to a depth of 3–2 km by ~260 Ma. Following Carminati et al. (2009), such exhumation could be related to late Hercynian orogenesis, expressed though uplift and erosion. In this case, this implies a total of ~3–4 km of denudation in the Kola Peninsula over ~60 million years, that is, a denudation rate as high as 50–100 m/Myr, which is more common for active orogenic belts.

The modern state of knowledge about Phanerozoic denudation of the Kola Peninsula is summarized in Hall (2015) and is based on a multifactor analysis of the thickness and location of offshore sedimentary deposits, as well as on morphology and petrographic features of the Devonian intrusions—alkaline and carbonatite massifs, dykes, and explosure pipes. In addition, Hall (2015) used a limited amount of published apatite and zircon fission track data. According to this study, high denudation rates are indeed recorded in the Phanerozoic history of the Kola Peninsula, but in the interval 400–360 Ma. At that time, up to 4 km of rocks were eroded from the central part of the Kola Peninsula and in the Kandalaksha Gulf area of the White Sea. However, the total denudation of the central and southwestern parts of the Kola Peninsula starting from 360 Ma up to present is estimated as ~2 km, that is, the average denudation rate during this time was ~5.6 m/Myr. In coastal areas of the Barents and White Seas, as well as close to the Russia-Finland border, the depth of the post-Devonian denudation is estimated to be less than 1 km (Hall, 2015). From this point of view, the direct interpretation of our AFT dating results and thermal models does not support the conclusions of Hall (2015).

On the other hand, after cessation of the Devonian magmatic event ~360 Ma, the Kola Peninsula area was thought to have been buried beneath relatively thick (>3 km) successions of sediments, causing resetting of AFT system. This scenario is well supported by numerous thermochronological studies from the Scandinavian countries (Kohn & Gleadow, 2019, and references therein) and is related to foreland basin development during the Caledonian collisional orogeny 430–390 Ma. According to the modern point of view, the scale of the Caledonian mountains can be compared with the Himalayas (Streule et al., 2010) such that the corresponding foreland basin could have been up to 300-km wide and ~6-km deep (Huigen & Andriessen, 2004; Samuelsson & Middleton, 1998). Moreover, Larson et al. (1999) report Paleozoic AFT partial annealing some 450–600 km east of the present Caledonide front. They interpreted this as an increase in paleotemperature due to Phanerozoic sediment burial connected with the development of a back bulge basin (the Baltic Devonian Basin), which is partly represented by cannibalized and redeposited sediments from the Caledonian foreland basin (Larson et al., 1999).

Our AFT data can be interpreted in the same way as FT data from Sweden and Finland (Kohn & Gleadow, 2019), if we assume that this back bulge basin extended to the Kola Peninsula area (the Kola back bulge basin) and then fully eroded. The presence of thick late Paleozoic and Mesozoic sedimentary successions in the southwestern Barents Sea—the Kola Monocline (Faleide et al., 2017; Henriksen et al., 2011)—supports this assumption.

5.2.2. Scenario #2: Slow Long-Term Cooling by Thermal Relaxation of the Upper Crust After the Middle-Late Devonian Magmatism

Alternatively, the rocks of the present-day surface of the Kola part of the Fennoscandian Shield may have experienced reheating to temperatures above 110 °C (the temperature of the complete annealing of fission tracks in apatite) owing to elevated heat flow associated with prolonged activity during formation of the Devonian alkaline magmatic province between 400 and 360 Ma. In this case, the thermochronology of the Kola Peninsula's upper crust in the 320–260 Ma interval can be characterized as follows:

1. U-Pb, Rb-Sr and Sm-Nd ages of the Devonian igneous complexes record the time of their intrusion and crystallization (400–375 Ma).
2. Plagioclase $^{40}Ar/^{39}Ar$ ages from the Devonian intrusions record the time since cooling below the plagioclase K-Ar closure temperature (~250 °C) from the youngest known $^{40}Ar/^{39}Ar$ age, is ~360 Ma.
3. Apatite fission track ages from the Kola Devonian intrusions and their host Precambrian rocks record the time of cooling of the present-day surface rocks to a temperature below 110 °C (320–280 Ma, on average 300 Ma).

Thus, according to scenario #2, the cooling time of the upper crust of the Kola Peninsula after cessation of the Kola Alkaline Province magmatism (360 Ma) to a temperature below 110 °C (~300 Ma) is ~60 Myr. The hypothesis of a long-term post-magmatic cooling of a large magmatic pluton has already been tested using the computer modeling for the purpose of tectonic interpretation of the AFT ages of the Khibina massif but was ruled out (Veselovskiy et al., 2015). In this study, we test an alternative hypothesis to explain long-term cooling of the Kola Peninsula upper crust after reheating by subcrustal intrusion.

5.2.3. Modeling of NE Fennoscandia Upper Crust Heating by a Subcrustal Heat Source

Here we aim to test the impact of regional heating due to either lower crust intrusion (underplating), similar to the Siberian traps case (Rosen et al., 2009) or a mantle plume effect on shallow depth (~3 km) crustal temperature. For this purpose, we perform modeling of the regional thermal history based on a 1-D numerical solution of the heat equation. This modeling allows us to provide constraints on plausible temperature range at given rocks properties and, additionally, first-order estimates on the reasonable timing of the proposed heating event.

For both performed experiments (Figure 6), crustal structure of the Kola part of Fennoscandia was set according to the data of the global crustal model Crust 2.0 (Bassin et al., 2000; Mooney et al., 1998). Given the generic nature of our numerical experiments, we used the most commonly excepted thermal parameters for the continental crust (Bittner & Schmeling, 1995; Clauser & Huenges, 1995).

Vertical spatial dimension of the models is 40 km. The model setup of the first experiment consists of a two-layer equally divided crust. Thermal conductivity is assumed to be constant (3 $W\ m^{-1}\ K^{-1}$) for both layers and density is 2.8 and 2.95 g/cm^3 for upper and lower crust respectively. The second model differs by the

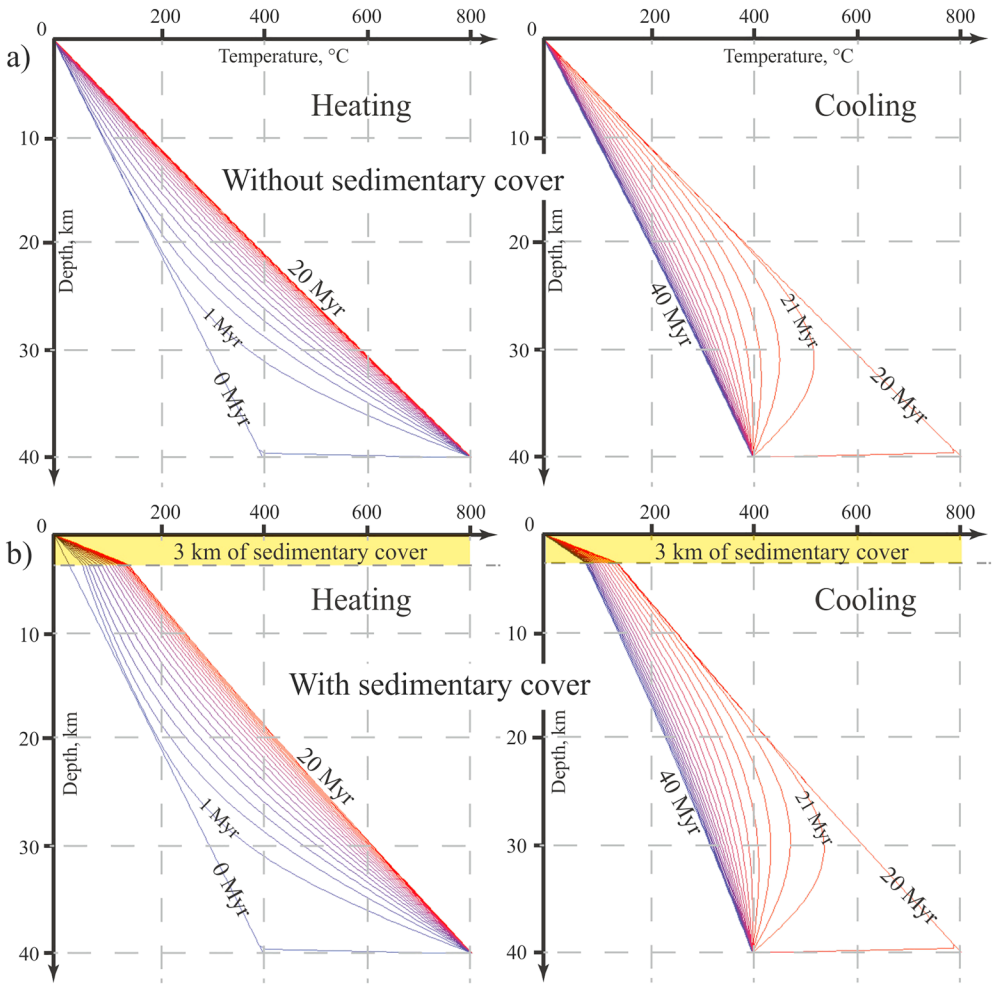

Figure 6. One-dimensional temperature distribution evolution for two experiments: without (a) and with (b) 3-km thick "sedimentary" layer at the top of the model. Color of the line refers to the time step from 0 (blue) to 20 (red) Myr.

presence of a 3.0-km thick top layer with material parameters typical for sedimentary rocks: density of 1.7 g/cm^3 and thermal conductivity of 1.0 W m^{-1} K^{-1}, that is, considerably decreased relative to the underlying layers. Low values of thermal conductivity (≤1.5 W m/K) are typical for high-porosity sedimentary rocks (Eppelbaum et al., 2014).

The initial temperature distribution in both cases is linear, from 0 °C at the surface to 400 °C at the Moho (Artemieva, 2006). Thermal impact due to deeper heat source is introduced into the models by thermal boundary condition at the model bottom, referring to fixed temperature of 800 °C. This aims to mimic instantaneous heating of subcrustal mantle associated to the emplacement of a plume head directly under the central part of the Kola Peninsula.

A steady state temperature distribution is reached in 16–20 million years for both models. For the first experiment (Figure 6a), resulting thermal distribution in the crust tends to be linear with the temperature of <50 °C in the depth interval of the first 3 km. Yet the implementation of the top "sedimentary" layer (second experiment, Figure 6b) leads to a significant increase in the temperature gradient within the upper-most part of the crust, with temperature of ~160 °C at a depth of 3 km. Thus, the thermal perturbation at the bottom of the crust can be reflected in anomalous high temperature at the shallow crustal level only in the context of thick sedimentary cover. These results are in general agreement with the study by Foulger (2010) and Łuszczak et al. (2017) showing rapidly increased geothermal gradient when the thermal conductivity of the blanketing layer is <2 W m/K.

5.2.4. Scenario #3: Increased Heat Flow in the Carboniferous.

According to the last proposed scenario for the Kola Peninsula thermal history, the events developed in the following sequence (Figure 5b).

1. 400–360 Ma—warming up of the upper crust during the formation of the Kola alkaline magmatic province;
2. 360–300 Ma—prolonged residence of the present-day surface rocks at shallow depths under conditions of increased heat flow in the temperature range 250–110 °C;
3. 300–260 Ma—cooling from 110 °C to 60–40 °C due to decreasing of heat flow.

Several possibilities exist to explain increased heat flow beneath the Kola Peninsula at this time. According to recent research (Arzamastsev et al., 2009, 2017; Marty et al., 1998), the Kola Alkaline Province was formed as a result of the plume-lithospheric interaction ~400–360 Ma. The depth of the magma generation zone beneath the Kola Alkaline Province is estimated at 80–120 km; a characteristic diameter of the plume head, defined from the area of alkaline magmatism manifestations, is estimated at 600 km (Arzamastsev et al., 2009). Obviously, this pattern could be a reason for elevated near surface heat flow resetting the AFT ages between 400 and 360 Ma. Paleotectonics also provides a possible source for additional heat flow in Carboniferous, 360–300 Ma. For example, a series of absolute, longitudinal and true polar wander corrected paleotectonic reconstructions of Baltica (Domeier & Torsvik, 2014) demonstrates (Figure 7), that 340–290 Ma the Kola part of Baltica drifted above the projection of a plume generation zone on the surface, which correlates with the edge of the African large low shear-wave velocity province "Tuzo" in the lowest mantle. This provides a potential source of increased heat flow, which caused warming of the rocks of the crystalline basement to temperatures above 110 °C, but not higher than 250 °C.

There is also some independent geological evidence for elevated heat flow at 360–300 Ma. This includes hydrothermal low- and medium-temperature Carboniferous veins with ore mineralization (Fedotova, 1990), although the date of these veins has not yet been verified using modern geochronology techniques. At the same time, the manifestations of Carboniferous-Permian magmatism are well known in the northern part of the East European Platform. Among them, alkaline-basaltic magmatism of the Oslo graben (~290–260 Ma), intrusive magmatism (dykes and sills of basic and alkaline rocks), observed in the sedimentary cover of the southeastern part of the Baltic and on the territory of the adjacent Baltic countries (335–305 Ma; Kharin & Eroshenko, 2007). In addition, Larson and Tullborg (1998) noted that discordant U-Pb ages of zircons from the Precambrian basement within Fennoscandia often have the lower intersection corresponding to ~300 Ma. This age is coeval with lead mobilization processes represented by low- and medium-temperature veins with lead mineralization. Increased mobility of lead is explained by the authors as a consequence of the heating of zircon, which is abundant in the rocks of the crystalline basement to the temperatures slightly above 110 °C in the presence of aqueous fluid (Larson & Tullborg, 1998).

Recent studies of the lithospheric structure across the Barents-Kara Sea region (Faleide et al., 2017) denote the presence of a high-density body at the crust-mantle transition under the East Barents Basin. This body is likely related to magmatism associated with Late Devonian rifting, the cooling of which caused a long-term subsidence of a basin now filled by thick sequences of pre-Permian sediments. Existence of such a large slowly cooling body beneath the Kola region crust agrees well with the obtained AFT data and the t-T model proposed.

5.2.5. A Synthesis of the Observed Thermal and Exhumation Models: Toward the Truth

Finally, we present one more scenario for the post-Devonian exhumation history of the Kola Peninsula area based mostly on the synthesis of the previous discussion. In this scenario, we propose the presence of the thick sedimentary and/or volcanic cover over NE Fennoscandia for a relatively long time after the end of the Devonian magmatism. Actually, the existence of a now-removed Late Devonian-Carboniferous sedimentary cover over the Kola area has been previously proposed by Nikishin et al. (1996). This suggestion is also based on lithological-facies characteristics of terrigenous rocks from the Main Devonian Field of the Russian sedimentary basin (Panova et al., 2003), according to which the "Baltic Shield" area was the only provenance of these red beds during the Frasnian and Famennian. Moreover, mineralogical composition (Panova et al., 2003) indicates that mafic rocks were the main source of these sediments. Taking into account the approximate area of the Upper Devonian terrigenous sedimentary deposits within the Main Devonian Field (~200,000 km^2) and their average thickness (~300 m), the total volume of mafic rocks, which must

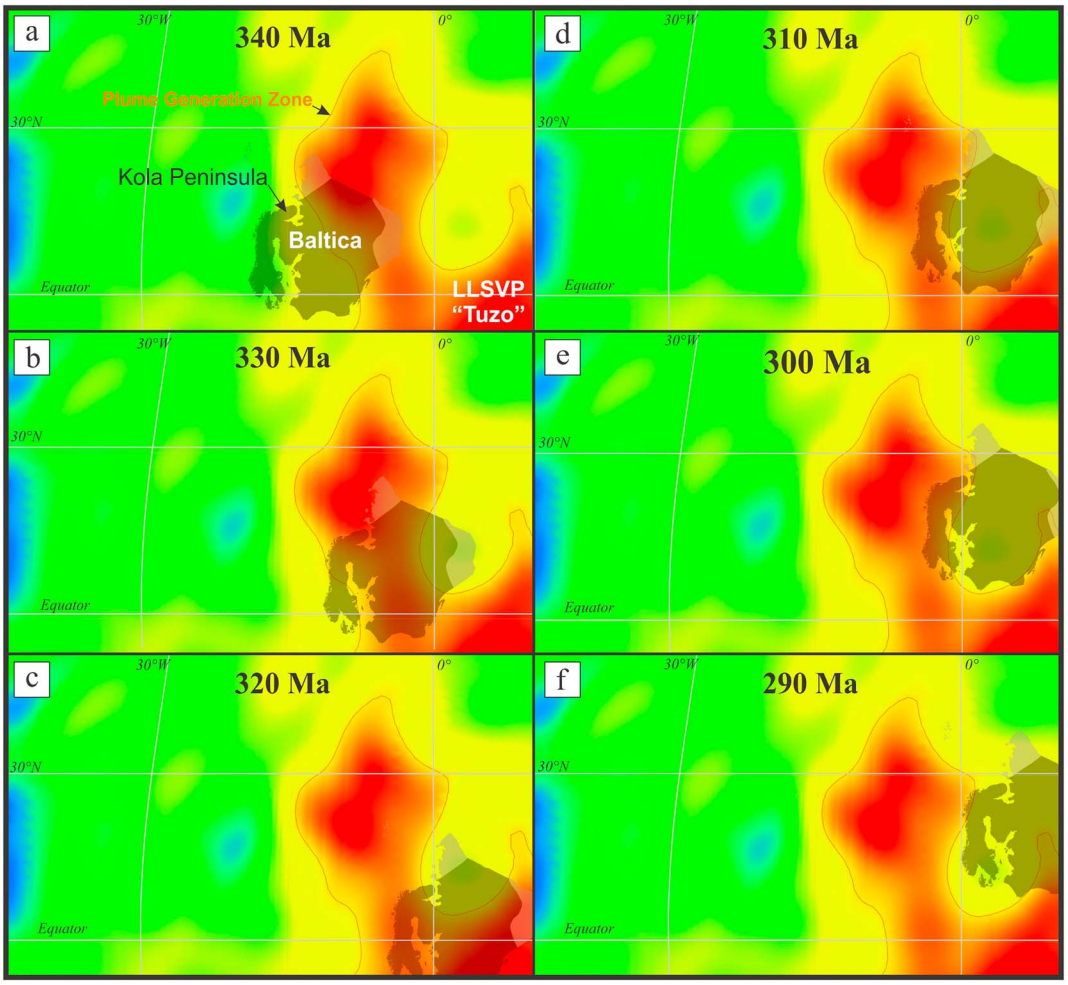

Figure 7. A series of absolute (longitudinal corrected) paleotectonic reconstructions of Baltica between 340 and 285 Ma according to the paleotectonic model of Domeier and Torsvik (2014). The color corresponds to the change in *S* wave velocities (Vs) according to the SMEAN tomographic model of the lower mantle at a depth of 2800 km (Becker & Boschi, 2002): red—zones of lower (>1%) relative to the model *S* wave velocities; green—conformity to model value; blue—zones of increased (>1%) *S* wave velocities. The figure also shows the contour (orange curve) of the "−1%" anomaly of the *S* waves, which is regarded as a plume generation zone. AFT = apatite fission track.

have been eroded from the northern Fennoscandia, can be estimated at ~60,000 km^3. Such first-order estimations suggest that the presence of a quite thick sequence of Devonian volcanics must have formerly overlain the Kola Peninsula area, with thickness reaching 1–2 km. If so, according to the proposed existence of a Kola "back-bulge" sedimentary basin (see section 5.2.1), numerical modeling (see section 5.2.3), and the evidence supporting elevated heat flow in Carboniferous (see section 5.2.4), the long-lasting period of residence of the present-day surface rocks at the increased temperatures beneath the sedimentary/volcanic cover would be enough to reset the AFT ages. This cover must have been partially removed in the Late Devonian-Carboniferous at the same time as the reduction in heat flow that caused rapid Permian cooling of the upper crust as distinctively recorded by t-T models that best predict the AFT data (Figures 4 and 5).

6. Conclusions

Results of this study, as well as previously published $^{40}Ar/^{39}Ar$ and apatite fission track ages from the Precambrian and Devonian rocks within the Kola Peninsula, taken together with the results of computer modeling of the thermal history of large plutons and rocks of the upper crust and independent estimates

of denudation from the studied area, have allowed us to synthetize a robust model for the thermal evolution over Paleoproterozoic and Phanerozoic time. The main conclusions of this work are as follows:

1. Since the end of the Paleoproterozoic, the thermal evolution of the NE Fennoscandia was characterized by a stable temperature regime: from 1.9 Ga until now the rocks of the present-day surface of the Kola part of Fennoscandia cooled monotonously at an average rate of ~0.15 °C/Myr, which is likely to be related to slow long-term exhumation at a rate of ~1–2 m/Myr. Numerous $^{40}Ar/^{39}Ar$ ages obtained for micas indicate that since 1.9 Ga, the present-day surface rocks have not experienced reheating above 350 °C. Our results suggest that Precambrian tectonic units of the Kola Peninsula, such as Central Kola and Murmansk terranes, have slightly different thermal history due to their internal heterogeneity.
2. Total denudation since 1.9 Ga is estimated by clinopyroxene geothermobarometry not to have exceeded ~3–5 km. First-order estimation of the early Proterozoic geothermal gradient, based this denudation depth and obtained $^{40}Ar/^{39}Ar$ thermochronology data, is ~75 °C/km.
3. Since the most recent active magmatic event about 360 and up to 300 Ma, crystalline basement rocks of Fennoscandia and Devonian intrusions currently exposed at the surface were located at depths 3 km or deeper and were heated to temperatures between 250 and 110 °C. This heating we relate to increased heat flow associated with drifting of NE Fennoscandia above the African superplume and/or thermal blanketing and burial caused by accumulation of low thermal conductivity Devonian-Carboniferous sedimentary/volcanic cover over the Kola Peninsula area. These results support the existence in the Phanerozoic history of the East European Platform of a prolonged stage of endogenous activity between 360 and 300 Ma. This conclusion is confirmed by results from the Kola Superdeep Borehole (SG3) using multidiffusion domain modeling of K-Feldspar $^{40}Ar/^{39}Ar$ data (Lovera, 1992). This previously "hidden" Carboniferous endogenous event is reflected in the disturbance of the U-Pb isotope system in zircons from the East European Craton basement, as well as in manifestations of basalt magmatism within the inner craton areas.

Acknowledgments
We thank two anonymous reviewers for their comments, which greatly improved our manuscript. This work was funded by the grant of Russian Science Foundation 16-17-10260, the grant of the Russian Government (#220, project 14.Z50.31.0017), the grant of President of Russian Federation MD1116.2018.5 and partly supported by the State scientific program of IPGG and IPE RAS and by the state assignment project of Sobolev Institute of Geology and Mineralogy, Siberian Branch of Russian Academy of Sciences 0330-2016-0013. All raw data used in this study are presented in the manuscript and in the supporting information (https://archive.org/details/TableS1Tectonics).

References

Amantov, A., Sederberg, P., & Hagenfeldt, S. (1995). The Mesoproterozoic to Lower Palaeozoic sedimentary bedrock sequence in the Northern Baltic Proper, Aland Sea, Gulf of Finland and Lake Ladoga. Prace Panstwow. Inst. Geol. CXLIX, Warsaw, 19–25.

Amantov, A. V., & Fjeldskaar, W. (2013). Geological-geomorphological features of the Baltic region and adjacent areas: Imprint on glacial-postglacial development. *Regionalnaya geologiya i metallogeniya*, *53*, 90–104. In Russian

Amelin, J. V., & Zaitsev, A. N. (2002). Precise geochronology of phoscorites and carbonatites: The critical role of U-series disequilibrium in age interpretations. *Geochimica et cosmochimica acta*, *66*(13), 2399–2419. https://doi.org/10.1016/S0016-7037(02)00831-1

Artemieva, I. M. (2006). Global 1×1 thermal model TC1 for the continental lithosphere: implications for lithosphere secular evolution. *Tectonophysics*, *416*(1-4), 245–277. https://doi.org/10.1016/j.tecto.2005.11.022

Arzamastsev, A. A., Arzamastseva, L. V., & Zaraiskiy, G. P. (2011). Contact Interaction of Agpaitic Magmas with Basement Gneisses: An Example of the Khibina and Lovozero Massifs. *Petrology*, *19*(2), 109–133. https://doi.org/10.1134/S0869591111020032

Arzamastsev, A. A., Fedotov, Z. A., & Arzamastseva, L. V. (2009). *Dyke Magmatism of the Northeastern Baltic Shield*. St.Petersburg: Nauka. in Russian

Arzamastsev, A. A., Glaznev, V. N., Raevsky, A. B., & Arzamastseva, L. V. (2000). Morphology and internal structure of the Kola Alkaline intrusions, NE Fennoscandian Shield: 3D density modelling and geological implications. *Journal of Asian Earth Sciences.*, *18*(2), 213–228. https://doi.org/10.1016/S1367-9120(99)00052-8

Arzamastsev, A. A., & Petrovsky, M. N. (2012). Alkaline volcanism in the Kola Peninsula, Russia: Paleozoic Khibiny, Lovozero and Kontozero calderas. *Proceedings of the MSTU*, *15*(2), 277–299.

Arzamastsev, A. A., Travin, A. V., Belyatskii, B. V., & Arzamastseva, L. V. (2003). Paleozoic Dike Series in the Kola Alkaline Province: Age and Characteristics of Mantle Sources. *Transactions (Doklady) of the Russian Academy of Sciences/Earth Science Section*, *391A*(6), 906–909.

Arzamastsev, A. A., Veselovskiy, R. V., Travin, A. V., Yudin, D. S., & Belyatsky, B. V. (2017). Paleozoic tholeiitic magmatism of the Kola Province: Areal distribution, ages, and relation to alkaline magmatism. *Petrology*, *1*(25), 42–65.

Arzamastsev, A. A., & Wu, F.-Y. (2014). U–Pb geochronology and Sr–Nd isotopic systematics of minerals from the ultrabasic alkaline massifs of the Kola Province. *Petrology*, *22*(5), 462–479. https://doi.org/10.1134/S0869591114050026

Balagansky, V. V., Glaznev, V. N., & Osipenko, L. G. (1998). Early Proterozoic evolution of the Northeastern Baltic shield: A terrane analysis. *Geotectonics*, *32*, 81–92.

Bassin, C., Laske, G., & Masters, G. (2000). The current limits of resolution for surface wave tomography in North America. *EOS Trans AGU*, *81*, 897.

Batieva, I. D. (1976). *Petrology of alkaline granites of the Kola Peninsula*. Leningrad: Nauka.

Becker, T. W., & Boschi, L. (2002). A comparison of tomographic and geodynamic mantle models. *Geochemistry, Geophysics, Geosystems*, *3*(1), 1003. https://doi.org/10.1029/2001GC000168

Bittner, D., & Schmeling, H. (1995). Numerical modelling of melting processes and induced diapirisms in the lower crust. *Geophysical Journal International*, *123*(1), 59–70. https://doi.org/10.1111/j.1365-246X.1995.tb06661.x

Carminati, E., Cuffaro, M., & Doglioni, C. (2009). Cenozoic uplift of Europe. *Tectonics*, *28*, TC4016. https://doi.org/10.1029/2009TC002472

Clauser, C., & Huenges, E. (1995). Thermal conductivity of rock and mineral. In *AGU Reference Shelf 3. Rock Physics & Phase Relations: A Handbook of Physical Constants*, (pp. 105–126). Washington. DC: American Geophysical Union.

Daly, J. S., Balagansky, V. V., Timmerman, M. J., Whitehouse, M. J., de Jong, K., Guise, P., et al. (2001). Ion microprobe U-Pb zircon geochronology and isotopic evidence for a trans-crustal suture in the Lapland–Kola Orogen, northern Fennoscandian Shield. *Precambrian Research*, *105*(2-4), 289–314. https://doi.org/10.1016/S0301-9268(00)00116-9

Daly, J.S., Timmerman, M.J., Balagansky, V.V., Bridgwater, D., & Marker, M. (1997). A telescoped passive margin to back-arc transition in the Lapland–Kola Orogen (LKO), northern Fennoscandian Shield. Abstr. Suppl., Terra Nova, 9, 129.

Domeier, M., & Torsvik, T. H. (2014). Plate tectonics in the late Paleozoic. *Geoscience Frontiers*, *5*(3), 303–350. https://doi.org/10.1016/j.gsf.2014.01.002

Early Precambrian of the Baltic Shield (2005). Saint-Petersburg, Nauka Publ. (In Russian).

Eppelbaum, L., Kutasov, I., & Pilchin, A. (2014). Investigating deep lithospheric structures. *Applied geothermics*, 269–391. https://doi.org/10.1007/978-3-642-34023-9_6

Faleide, J. I., Pease, V., Curtis, M., Klitzke, P., Minakov, A., Scheck-Wenderoth, M., et al. (2017). Tectonic implications of the lithospheric structure across the Barents and Kara shelves. *Geological Society, London, Special Publications.*, *460*(1), 285–314. https://doi.org/10.1144/SP460.18

Fedotov, Z. A., Bayanova, T. B., & Serov, P. A. (2012). Spatiotemporal relationships of dike magmatism in the Kola Region, The Fennoscandian shield. *Geotectonics*, *46*(6), 412–426. https://doi.org/10.1134/S0016852112060039

Fedotova, M. G. (1990). *Caledonian vein mineralization of the Murmansk and White Sea coasts of the Kola Peninsula*. Apatity: Publishing house KSC of the USSR. in Russian

Flowers, R. M., Mahan, K. H., Bowring, S. A., Williams, M. L., Pringle, M. S., & Hodges, K. V. (2006). Multistage exhumation and juxtaposition of lower continental crust in the western Canadian Shield: Linking high-resolution U-Pb and $^{40}Ar/^{39}Ar$ thermochronometry with pressure-temperature-deformation paths. *Tectonics*, *25*, TC4003. https://doi.org/10.1029/2005TC001912

Fossen, H., Ksienzyk, A. K., & Jacobs, J. (2017). Correspondence: Challenges with dating weathering products to unravel ancient landscapes. *Nature Communications*, *8*(1), 1502. https://doi.org/10.1038/s41467-017-01457-9

Foulger, G. R. (2010). *Plates vs plumes: A geological controversy*. Hoboken, NJ: Wiley-Blackwell. https://doi.org/10.1002/9781444324860

Galbraith, R. F. (2005). *Statistics for fission track analysis*. Boca Raton: Chapman & Hall/CRC. https://doi.org/10.1201/9781420034929

Galbraith, R. F., & Laslett, G. M. (1993). Statistical models for mixed fission track ages. *Nuclear Tracks*, *21*, 459–470.

Gleadow, A. J. W. (1981). Fission-track dating methods: What are the real alternatives? *Nuclear Tracks*, *5*(1-2), 3–14. https://doi.org/10.1016/0191-278X(81)90021-4

Glebovitsky, V. A. (1997). *The Early Precambrian of Russia*. Amsterdam: Harwood Academic Publ.

Hall, A. M. (2015). Phanerozoic denudation across the Kola Peninsula, Northwest Russia: Implications for long-term stability of Precambrian shield margins. *Norwegian Journal of Geology*, *95*, 153–169.

Hendriks, B., Andriessen, P., Huigen, Y., Leighton, C., Redfield, T., Murrell, G., et al. (2007). A fission track data compilation for Fennoscandia. *Norwegian Journal of Geology*, *87*, 143–155.

Henriksen, E., Ryseth, A. E., Larssen, G. B., Heide, T., Rønning, K., Sollid, K., & Stoupakova, A. V. (2011). Tectonostratigraphy of the greater Barents Sea: Implications for petroleum systems. *Geological Society, London, Memoirs*, *35*(1), 163–195. https://doi.org/10.1144/m35.10

Huhma, H., & Meriläinen, K. (1991). Provenance of paragneisses from the Lapland Granulite Belt. abstract. In P. Tuisku, & K. Laajoki (Eds.), *Metamorphism, deformation and structure of the crust, les. Terrae. Ser. A, No. 5*, (p. 26). Oulu, Finland: University of Oulu.

Huigen, Y., & Andriessen, P. (2004). Thermal effects of Caledonian foreland basin formation, based on fission track analyses applied on basement rocks in central Sweden. *Physics and Chemistry of the Earth*, *29*(10), 683–694. https://doi.org/10.1016/j.pce.2004.03.006

Hurford, A. J. (1990). Standardization of fission track dating calibration: Recommended by the Fission Track Working Group of the I.U.G.S. Subcommission on Geochronology. *Chemical Geology*, *80*(2), 171–178.

Hurford, A. J., & Green, P. F. (1983). The Zeta-Age Calibration of Fission-Track Dating. *Isotope Geoscience*, *1*, 285–317.

Japsen, P., Green, P. F., Bonow, J. M., & Erlström, M. (2016). Episodic burial and exhumation of the southern Baltic Shield: Epeirogenic uplifts during and after break-up of Pangaea. *Gondwana Research*, *35*, 357–377. https://doi.org/10.1016/j.gr.2015.06.005

Ketcham, R. A. (2005). Forward and inverse modeling of low-temperature thermochronometry data. *Reviews in Mineralogy and Geochemistry*, *58*(1), 275–314. https://doi.org/10.2138/rmg.2005.58.11

Ketcham, R. A., Carter, A., Donelick, R. A., Barbarand, J., & Hurford, A. J. (2007). Improved modeling of fission-track annealing in apatite. *American Mineralogist*, *92*(5-6), 799–810. https://doi.org/10.2138/am.2007.2281

Kharin, G. S., & Eroshenko, D. V. (2007). *The basaltoid of the Baltic is a possible link between the magmatism of the Oslo graben and the Pripyat-Donetsk avlakogen (geochemistry, genesis, evolution). Alkaline magmatism of the Earth and its ore-bearing. Mat. Intern. Meeting*. Kiev: NAS. in Russian

Kogarko, L. N., Kononova, V. A., Orlova, M. P., & Woolley, A. R. (1995). Alkaline rocks and carbonatites of the world. 2. Former USSR (p. 232). London, UK: Chapman & Hall. https://doi.org/10.1007/978-94-010-909

Kohn, B., & Gleadow, A. (2019). Application of low-temperature thermochronology to craton evolution. Chapter 21. In M. G. in Malusa, & P. G. Fitzgerald (Eds.), *Fission track thermochronology and its Application to Geology*, (pp. 373–393). Cham: Springer. https://doi.org/10.1007/978-3-319-89421-8_21

Kola Superdeep (1998). Scientific Results and Research Experience. In V. P. Orlov & N. P. Laverov, Moscow, TECHNONEFTEGAZ (260 p.) (In Russian).

Kozlov, E. N., & Arzamastsev, A. A. (2015). Petrogenesis of metasomatic rocks in the fenitized zones of the Ozernaya Varaka alkaline ultrabasic complex, Kola Peninsula. *Petrology*, *23*(1), 45–67. https://doi.org/10.1134/S0869591115010026

Kramm, U., & Kogarko, L. N. (1994). Nd and Sr isotope signatures of the Khibina and Lovozero agpaitic centres, Kola Alkaline Province, Russia. *Lithos*, *32*(3-4), 225–242. https://doi.org/10.1016/0024-4937(94)90041-8

Kramm, U., Kogarko, L. N., Kononova, V. A., & Vartiainen, H. (1993). The Kola alkaline province of the CIS and Finland: Precise Rb-Sr ages define 380–360 age range for all magmatism. *Lithos*, *30*(1), 33–44. https://doi.org/10.1016/0024-4937(93)90004-V

Ksienzyk, A. K., Dunkl, I., Jacobs, J., Fossen, H., & Kohlmann, F. (2014). From orogen to passive margin: Constraints from fission track and (U-Th)/He analyses on Mesozoic uplift and fault reactivation in SW Norway. *Geological Society, London, Special Publications*, *390*(1), 679–702. https://doi.org/10.1144/SP390.27

Kudryashov, N. M., Petrovsky, M. N., Mokrushin, A. V., & Elizarov, D. V. (2013). Neoarchean sanukitoid magmatism in the Kola region: Geological, petrochemical, geochronological, and isotopic-geochemical data. *Petrology*, *21*(4), 351–374. https://doi.org/10.1134/S0869591113030041

Larson, S. A., Tullborg, E., Cederbom, C., Björklund, L., Plink-Björklund, P., & Stiberg, J.-P. (1999). The Caledonian foreland basin in Scandinavia: Constrained by the thermal maturation of the Alum Shale. Final remarks. *GFF*, *121*(3), 269–270. https://doi.org/10.1080/11035899901213269

Larson, S. A., & Tullborg, E.-L. (1998). Why Baltic shield zircons yield late Paleozoic lower-intercept ages on U-Pb Concordia. *Geology*, *26*(10), 919–922. https://doi.org/10.1130/0091-7613(1998)026<0919:WBSZYL>2.3.CO;2

Lovera, O. M. (1992). Computer programs to model 40Ar/39Ar diffusion data from multidomain samples. *Computers & Geosciences*, *18*(7), 789–813.

Lovera, O. M., Richter, F. M., & Harrison, T. M. (1989). The $^{40}Ar/^{39}Ar$ thermochronometry for slowly cooled samples having a distribution of diffusion domain sizes. *Journal of Geophysical Research*, *94*(B12), 17,917–17,935. https://doi.org/10.1029/JB094iB12p17917

Łuszczak, K., Persano, C., Braun, J., & Stuart, F. M. (2017). How local crustal thermal properties influence the amount of denudation derived from low-temperature thermochronometry. *Geology*, *45*(9), 779–782. https://doi.org/10.1130/G39036.1

Marty, B., Tolstikhin, I., Kamensky, I. L., Nivin, V. A., Balaganskaya, E. G., & Zimmermann, J.-L. (1998). Plume-derived rare gases in 380 Ma carbonatites from the Kola region (Russia) and the argon isotopic composition in the deep mantle. *Earth and Planetary Science Letters*, *164*(1-2), 179–192. https://doi.org/10.1016/S0012-821X(98)00202-7

Melezhik, V. A., & Hanski, E. J. (2012). The Early Palaeoproterozoic of Fennoscandia: Geological and tectonic settings. In V. Melezhik, A. R. Prave, A. E. Fallick, L. R. Kump, H. Strauss, A. Lepland, & E. J. Hanski (Eds.), *Reading the archive of Earth's oxygenation. Vol. 1: The Palaeoproterozoic of Fennoscandia as context for the Fennoscandian Arctic Russia—Drilling Early Earth Project*, (pp. 33–38). Berlin Heidelberg: Springer-Verlag.

Mitrofanov, F. P., Pozhilenko, V. I., Smolkin, V. F., Arzamastsev, A. A., Yevzerov, V. Y., Lyubtsov, V. V., et al. (1995). *Geology of the Kola Peninsula*. Apatity: Kola Science Centre.

Mooney, A., Laske, G., & Masters, G. (1998). Crust 5.1: A global crustal model at 5x5 degrees. *Journal Geophysical Research*, *103*(B1), 727–747. https://doi.org/10.1029/97JB02122

Murrell, G. R. (2003). *The long-term thermal evolution of central Fennoscandia, revealed by integrated low temperature thermochronometry*. Amsterdam: Netherlands Research School of Sedimentary Geology.

Murrell, G. R., & Andriessen, P. A. M. (2004). Unravelling a long-term multi-event thermal record in the cratonic interior of southern Finland through apatite fission track thermochronology. *Physics and Chemistry of the Earth*, *29*(10), 695–706. https://doi.org/10.1016/j.pce.2004.03.007

Nikishin, A. M., Ziegler, P. A., Stephenson, R. A., Cloetingh, S. A. P. L., Furne, A. V., Fokin, P. A., et al. (1996). Late Precambrian to Triassic history of the East European Craton: Dynamics of sedimentary basin evolution. *Tectonophysics*, *268*(1-4), 23–63. https://doi.org/10.1016/S0040-1951(96)00228-4

Nimis, P. (1999). Clinopyroxene geobarometry of magmatic rocks. Part 2. Structural geobarometers for basic to acid, tholeiitic and mildly alkaline magmatic systems. *Contributions to Mineralogy and Petrology*, *135*(1), 62–74. https://doi.org/10.1007/s004100050498

Nosova, A. A., Larionova, Y. O., Travin, A. V., Kargin, A. V., & Dubinina, E. O. (2015). Rb-Sr and $^{40}Ar/^{39}Ar$ age of oranges in Kostomuksha (Western Karelia): Problems of dating of orangeites and lamproites. In *Isotope dating of geological processes: New results, approaches and perspectives. Materials of the VI Russian Conference on isotope geochronology. June 2-5, 2015* (pp. 198–200). St. Petersburg: IGGD of the Russian Academy of Sciences. - SPb: Sprinter. In Russian

O'Brien, H., Phillips, D., & Spencer, R. (2007). Isotopic ages of Lentiira-Kuhmo-Kostomuksha olivine lamproite—Group II kimberlites. *Bulletin of the Geological Society of Finland*, *79*(2), 203–215. https://doi.org/10.17741/bgsf/79.2.004

Panova, E. G., Kazak, A. P., & Yakobson, K. E. (2003). Terrigenous sedimentation on the Main Devonian field. *Lithosphere*, *4*, 19–31. in Russian

Peulvast, J.-P., Bétard, F., & Lageat, Y. (2009). Long-term landscape evolution and denudation rates in shield and platform areas: A morphostratigraphic approach. *Geomorphologie*, *2*, 95–108.

Putirka, K. D. (2008). Thermometers and barometers for volcanic systems. *Reviews in Mineralogy and Geochemistry*, *69*(1), 61–120. https://doi.org/10.2138/rmg.2008.69.3

Redfield, T. F., Braathen, A., Gabrielsen, R. H., Osmundsen, P. T., Torsvik, T. H., & Andriessen, P. A. M. (2005). Late Mesozoic to Early Cenozoic components of vertical separation across the Møre-Trøndelag Fault Complex, Norway. *Tectonophysics*, *395*(3-4), 233–249. https://doi.org/10.1016/j.tecto.2004.09.012

Reiners, P. W., Ehlers, T. A., & Zeitler, P. K. (2005). Past, present, and future of thermochronology. *Reviews in Mineralogy and Geochemistry*, *58*(1), 1–18. https://doi.org/10.2138/rmg.2005.58.1

Rohrman, M. (1995). *Thermal evolution of the Fennoscandian region from fission track thermochronology—An integrated approach*. PhD thesis. Amsterdam, 168: Vrije Universiteit Amsterdam.

Rosen, O. M., Soloviev, A. V., & Zhuravlev, D. Z. (2009). Thermal evolution of the northeastern Siberian platform in the light of apatite fission-track dating of the deep drill core. *Izvestiya. Physics of the Solid Earth*, *45*(10), 914–931. https://doi.org/10.1134/S1069351309100085

Rukhlov, A. S., & Bell, K. (2010). Geochronology of carbonatites from the Canadian and Baltic Shields, and the Canadian Cordillera: Clues to mantle evolution. *Mineralogy and Petrology*, *98*(1-4), 11–54. https://doi.org/10.1007/s00710-009-0054-5

Samuelsson, J., & Middleton, M. F. (1998). The Caledonian foreland basin in Scandinavia: Constrained by the thermal maturation of the Alum Shale. *GFF*, *120*(3), 307–314. https://doi.org/10.1080/11035899809453224

Sandström, B., Tullborg, E. L., Larson, S. Å., & Page, L. (2009). Brittle tectonothermal evolution in the Forsmark area, central Fennoscandian Shield, recorded by paragenesis, orientation and $^{40}Ar/^{39}Ar$ geochronology of fracture minerals. *Tectonophysics*, *478*(3–4), 158–174. https://doi.org/10.1016/j.tecto.2009.08.006

Sharkov, E. V., & Smolkin, V. F. (1997). The early Proterozoic Pechenga-Varzuga Belt—A case of Precambrian back-arc spreading. *Precambrian research*, *82*(1-2), 133–151. https://doi.org/10.1016/S0301-9268(96)00041-1

Sitnikova, M. A., Zaitsev, A. N., Wall, F., Chakhmouradian, A. R., & Subbotin, V. V. (2001). Evolution of chemical composition of rock-forming carbonates in Sallanlatvi carbonatites, Kola Peninsula, Russia. *Journal of African Earth Science*, *32*(l), 34–45.

Söderlund, P., Page, L. M., & Söderlund, U. (2008). $^{40}Ar-^{39}Ar$ biotite and hornblende geochronology from the Oskarshamn area, SE Sweden: Discerning multiple Proterozoic tectonothermal events. *Geological Magazine*, *145*(6), 790–799. https://doi.org/10.1017/S0016756808005001

Streule, M. J., Strachan, R. A., Searle, M. P., & Law, R. D. (2010). Comparing Tibet-Himalayan and Caledonian crustal architecture, evolution and mountain building processes. *Geological Society, London, Special Publications.*, *335*(1), 207–232. https://doi.org/10.1144/sp335.10

Vermeesch, P., & Tian, Y. (2014). Thermal history modelling: HeFTy vs. QTQt. *Earth-Science Reviews*, *139*, 279–290. https://doi.org/10.1016/j.earscirev.2014.09.010

Veselovskiy, R., Thomson, S. N., Arzamastsev, A. A., & Zakharov, V. S. (2015). Apatite fission track thermochronology of Khibina massif (Kola Peninsula, Russia): Implications for post-Devonian tectonics of the NE fennoscandia. *Tectonophysics*, *665*, 157–163. https://doi.org/10.1016/j.tecto.2015.10.003

Veselovskiy, R. V., Arzamastsev, A. A., Demina, L. I., Travin, A. V., & Botsyun, S. B. (2013). Paleomagnetism, geochronology, and magnetic mineralogy of Devonian dikes from the Kola alkaline province (NE Fennoscandian shield). *Izvestiya*. *Physics of the Solid Earth*, *49*(4), 526–547. https://doi.org/10.1134/S106935131303018X

Veselovskiy, R. V., Bazhenov, M. L., & Arzamastsev, A. A. (2016). Paleomagnetism of Devonian dykes in the northern Kola Peninsula and its bearing on the apparent polar wander path of Baltica in the Precambrian. *Tectonophysics*, *675*, 91–102. https://doi.org/10.1016/j.tecto.2016.03.014

Veselovskiy, R. V., Samsonov, A. V., Stepanova, A. V., Salnikova, E. B., Larionova, Y. O., Travin, A. V., et al. (2019). 1.86 Ga Key Paleomagnetic Pole from the Murmansk craton intrusions—Eastern Murman Sill Province, NE Fennoscandia: Multidisciplinary approach and paleotectonic applications. *Precambrian Research*, *324*, 126–145. https://doi.org/10.1016/j.precamres.2019.01.017

Vetrin, V. R. (2014). Duration of the formation and sources of the granitoids of the Litsk-Araguba Complex, Kola Peninsula. *Geochemistry International*, *52*(1), 33–45. https://doi.org/10.1134/S0016702914010091

Vetrin, V. R., Bayanova, T. B., Kamenskii, I. L., & Ikorskii, S. V. (2002). U-Pb ages and heliumisotope geochemistry of rocks and minerals from the Litsk-Aragubdiorite-granite complex (Kola Peninsula). *Doklady Earth Sciences*, *387*(8), 947–950.

Vetrin, V. R., Delenitsyn, A. A., Turkina, O. M., & Ludden, J. (2003). Geochemistry and reconstruction of the protolith composition of the basement of the Pechenga paleorift. *Petrology*, *11*(2), 177–204.

Vetrin, V. R., & Rodionov, N. V. (2009). Geology and geochronology of Neoarchean Anorogenic magmatism of the Keivy structure, Kola Peninsula. *Petrology*, *17*(6), 537–557. https://doi.org/10.1134/S0869591109060022

Wiersberg, T. (2001). Edelgase als Tracer für Wechselwirkungen von Krusten- und Mantelfluiden mit diamantführenden Gesteinen des östlichen Baltischen Schildes. PhD Dissertation, University of Postdam, 113 p.

Zachos, J., Pagani, M., Sloan, L., Thomas, E., & Billups, K. (2001). Trends, rhythms, and aberrations in global climate 65 Ma to present. *Science*, *292*(5517), 686–693. https://doi.org/10.1126/science.1059412

Zachos, J. C., Dickens, G. R., & Zeebe, R. E. (2008). An early Cenozoic perspective on greenhouse warming and carbon-cycle dynamics. *Nature*, *451*(7176), 279–283. https://doi.org/10.1038/nature06588